附錄 A

不同粒徑膠體粒子在不同濃度電解質溶液的 zeta potential

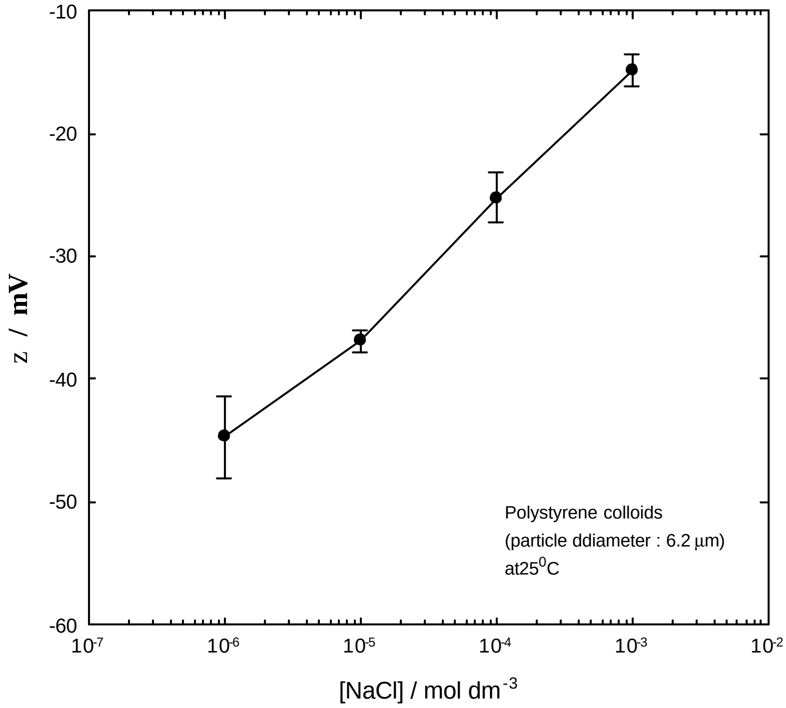

Fig[A-1] Plots of the zeta potential values for polystyrene colloids (particle diameter: 6.2µm)at 25^{o}C, as a function of the electrolyte (NaCl) concentration.

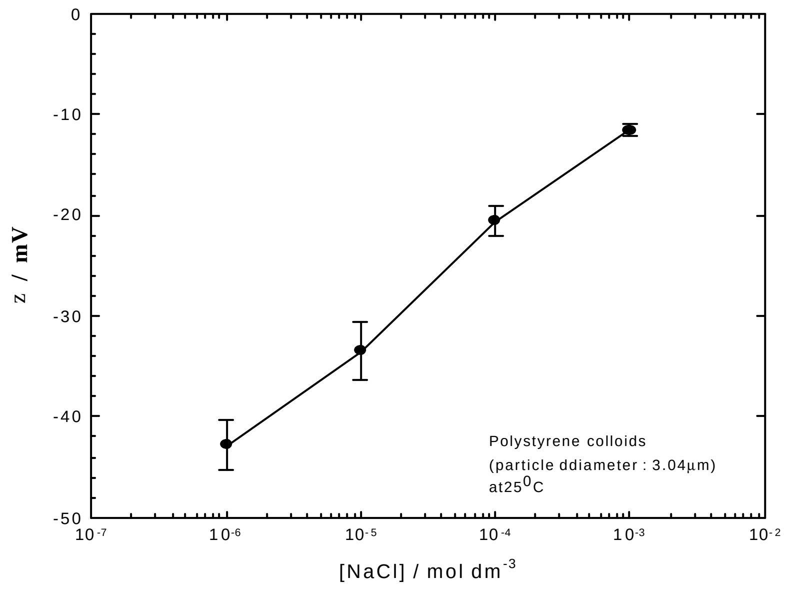

Fig[A-2] Plots of the zeta potential values for polystyrene colloids (particle diameter: 3.04µm)at 25^{o}C, as a function of the electrolyte (NaCl) concentration.

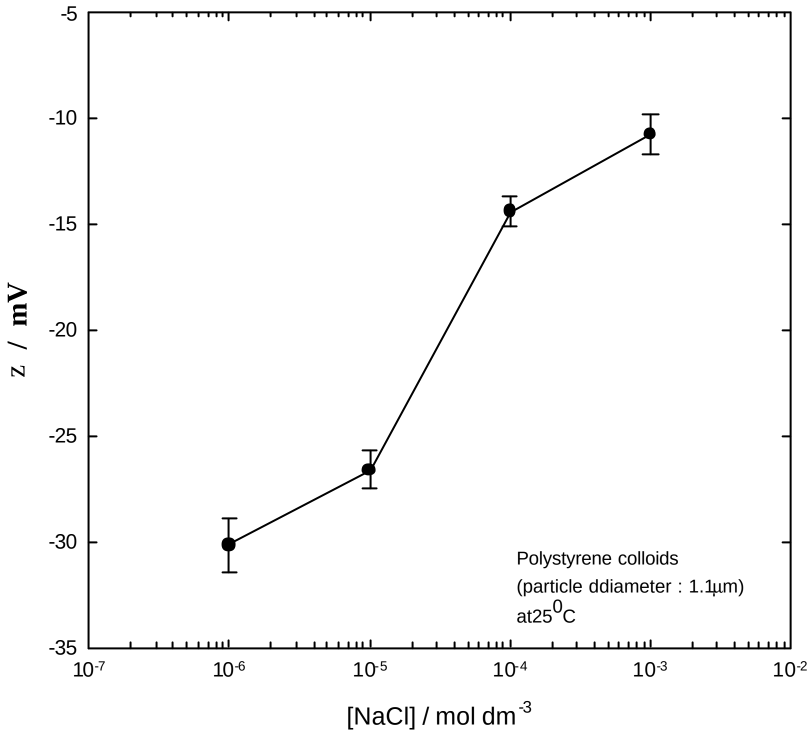

Fig[A-3] Plots of the zeta potential values for polystyrene colloids (particle diameter: 1.1μm)at 25°C, as a function of the electrolyte (NaCl) concentration.

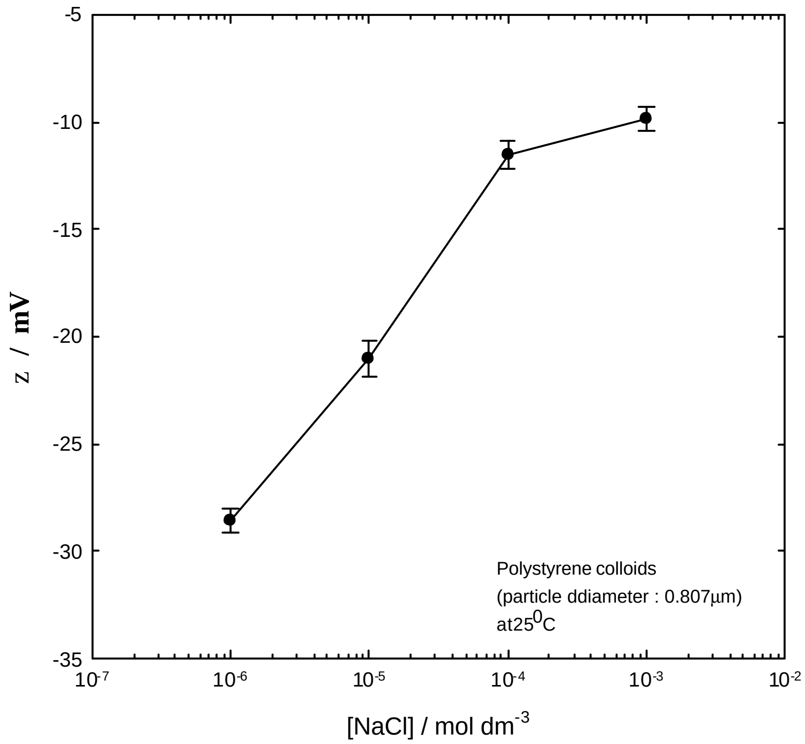

Fig[A-4] Plots of the zeta potential values for polystyrene colloids (particle diameter: 0.807μm)at 25°C, as a function of the electrolyte (NaCl) concentration.

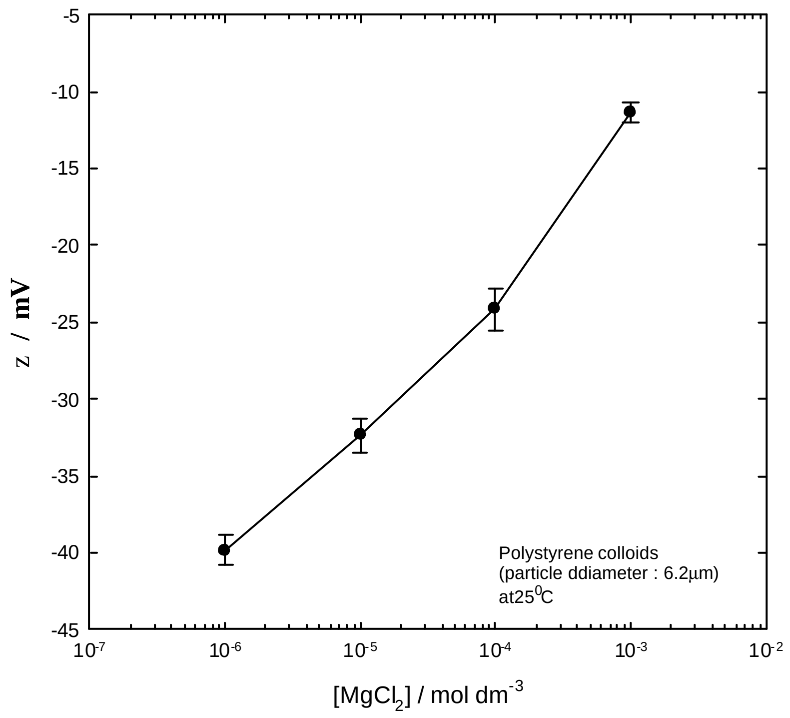

Fig[A-5] Plots of the zeta potential values for polystyrene colloids (particle diameter: 6.2μm)at 25^{o}C, as a function of the electrolyte ($MgCl_2$) concentration.

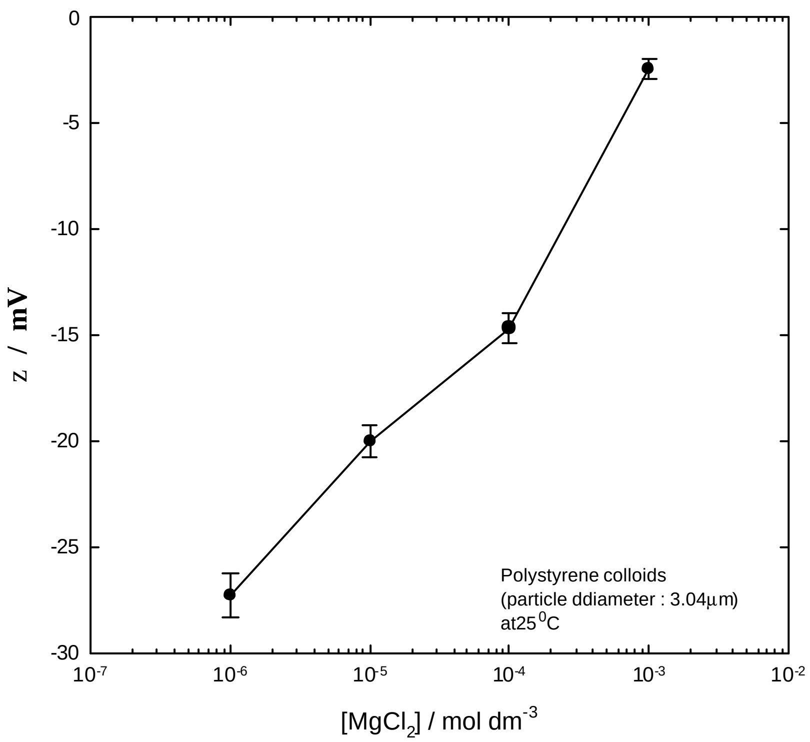

Fig[A-6] Plots of the zeta potential values for polystyrene colloids (particle diameter: 3.04μm)at 25^{o}C, as a function of the electrolyte ($MgCl_2$) concentration.

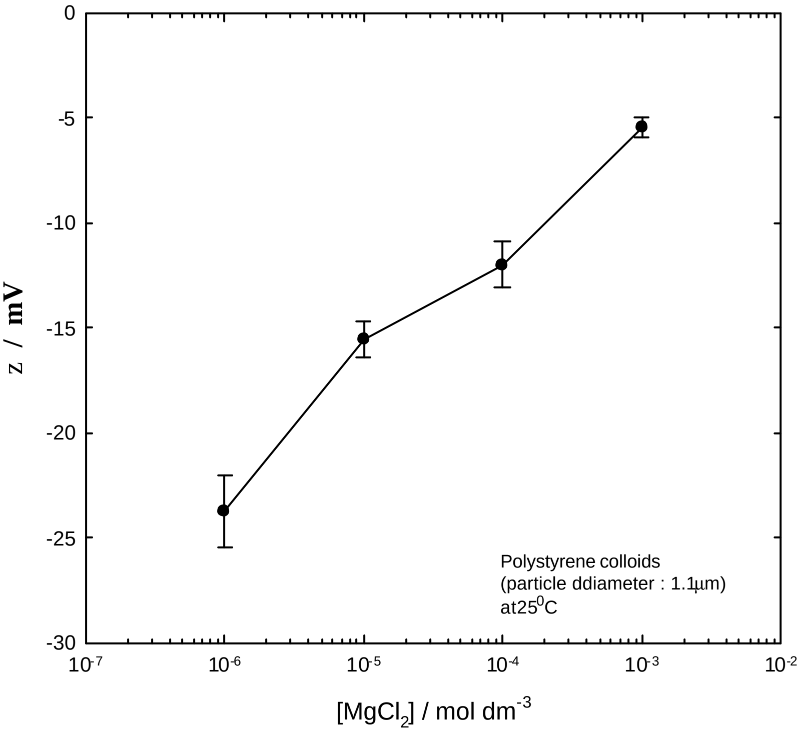

Fig[A-7] Plots of the zeta potential values for polystyrene colloids (particle diameter: 1.1μm)at 25°C, as a function of the electrolyte ($MgCl_2$) concentration.

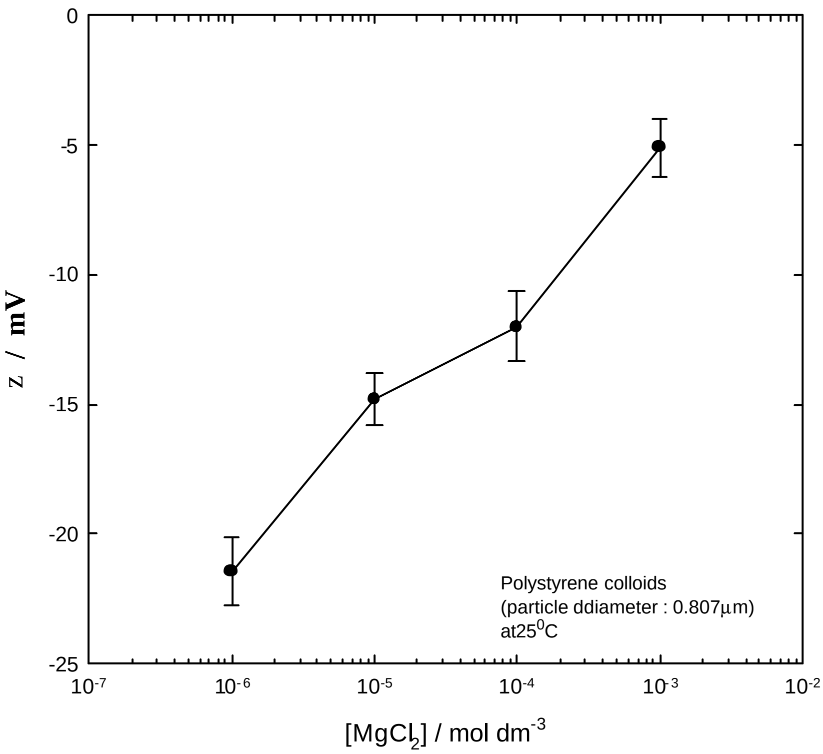

Fig[A-8] Plots of the zeta potential values for polystyrene colloids (particle diameter: 0.807μm)at 25°C, as a function of the electrolyte ($MgCl_2$) concentration.

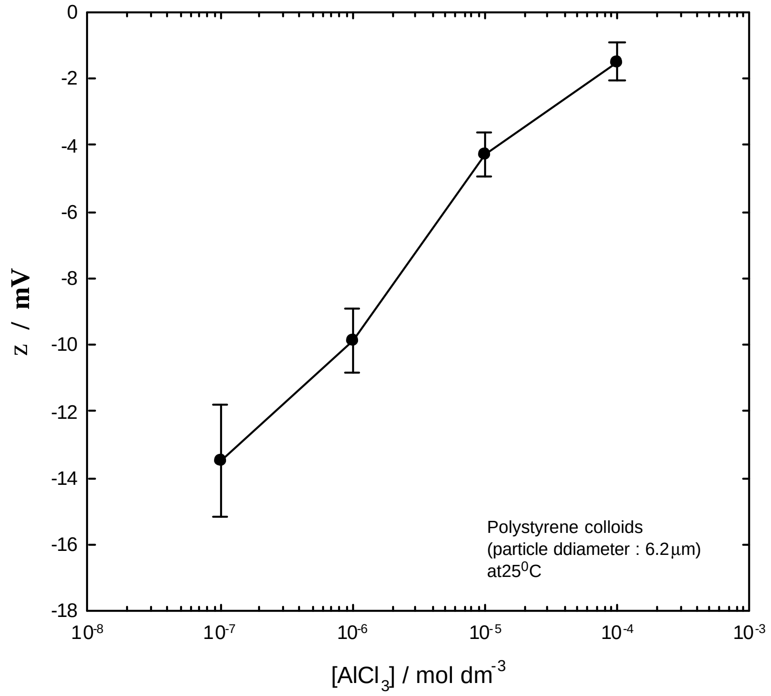

Fig[A-9] Plots of the zeta potential values for polystyrene colloids (particle diameter: 6.2μm)at 25^{o}C, as a function of the electrolyte ($AlCl_3$) concentration.

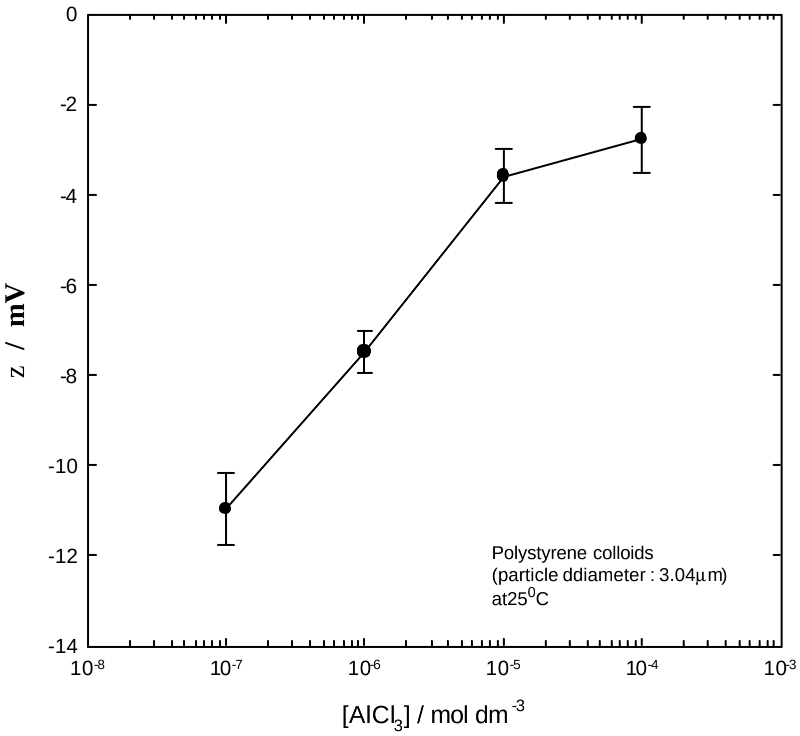

Fig[A-10] Plots of the zeta potential values for polystyrene colloids (particle diameter: 3.04μm)at 25^{o}C, as a function of the electrolyte ($AlCl_3$) concentration.

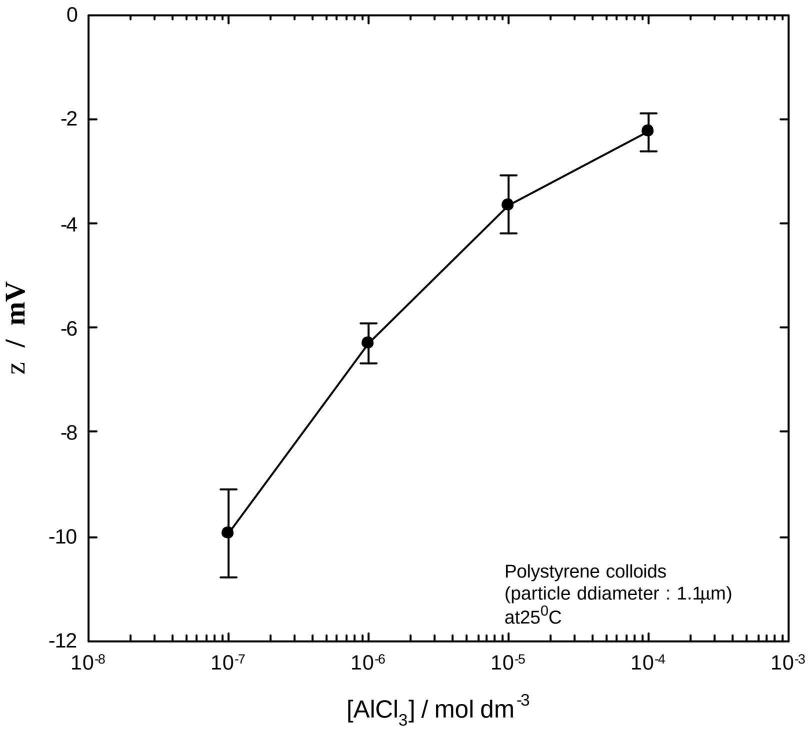

Fig[A-11] Plots of the zeta potential values for polystyrene colloids (particle diameter: 1.1μm)at 25^{o}C, as a function of the electrolyte ($AlCl_3$) concentration.

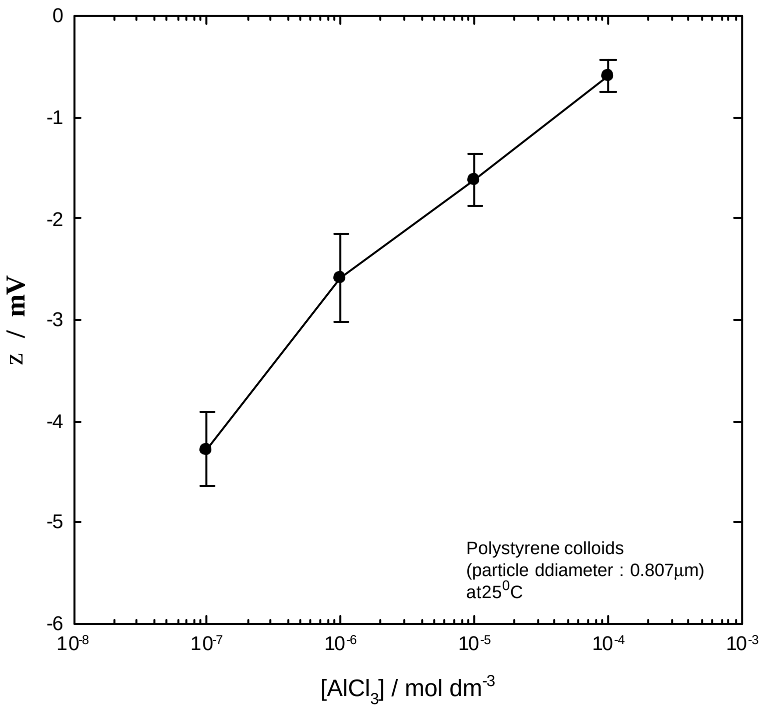

Fig[A-12] Plots of the zeta potential values for polystyrene colloids (particle diameter: 0.807μm)at 25^{o}C, as a function of the electrolyte ($AlCl_3$) concentration.

附錄 B

由 DLVO 理論計算不同粒徑膠體之全位能曲線

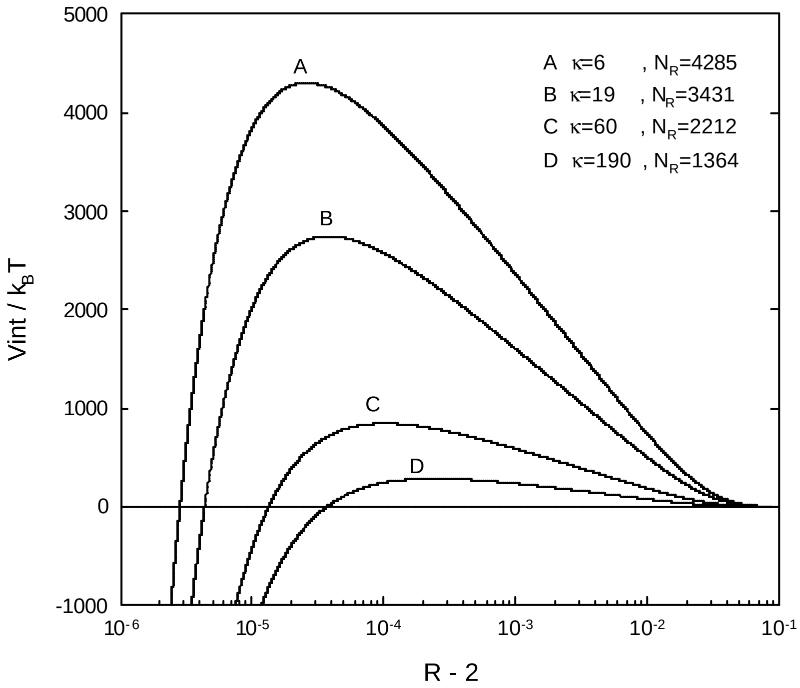

Fig[B-1] Schematic diagram of total interparticle potential energy curves for NaCl when particle diameters are at 1.1 μm and 6.2 μm, respectively。

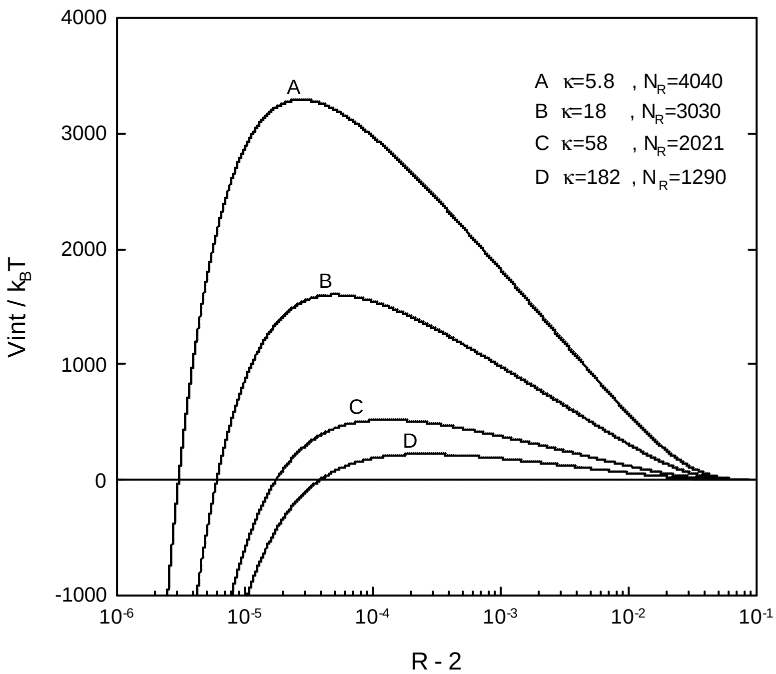

Fig[B-2] Schematic diagram of total interparticle potential energy curves for NaCl when particle diameters are at 0.807 μm and 6.2 μm, respectively。

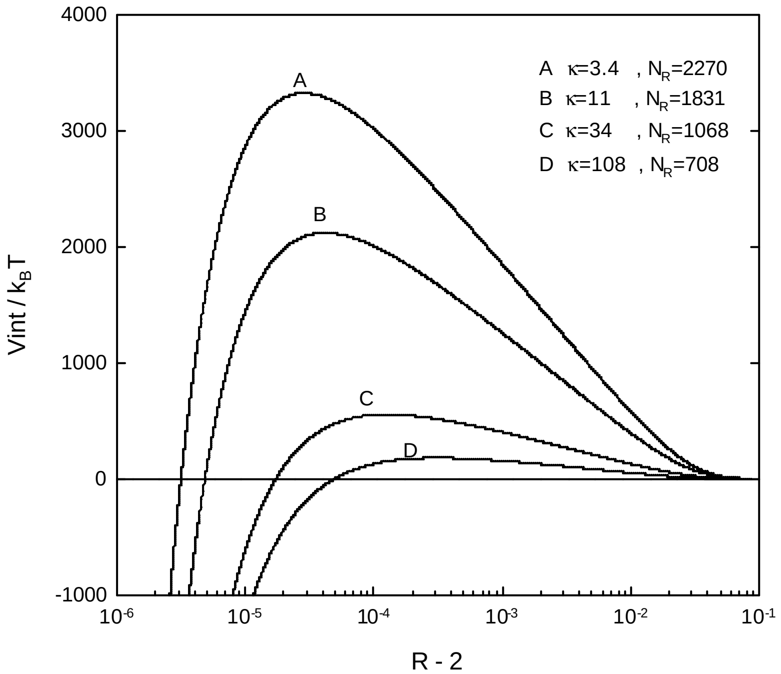

Fig[B-3] Schematic diagram of total interparticle potential energy curves for NaCl when particle diameters are at 1.1 μm and 3.04 μm, respectively。

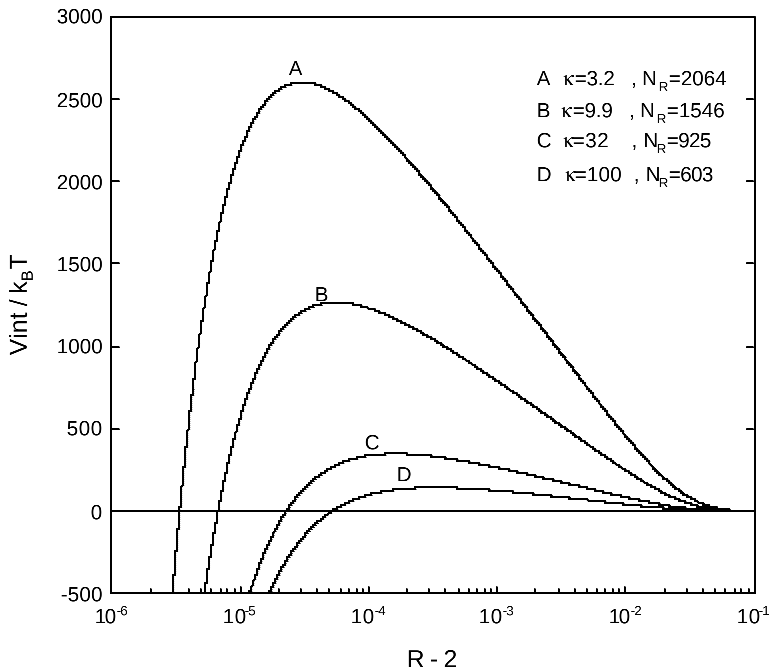

Fig[B-4] Schematic diagram of total interparticle potential energy curves for NaCl when particle diameters are at 0.807 μm and 3.04 μm, respectively。

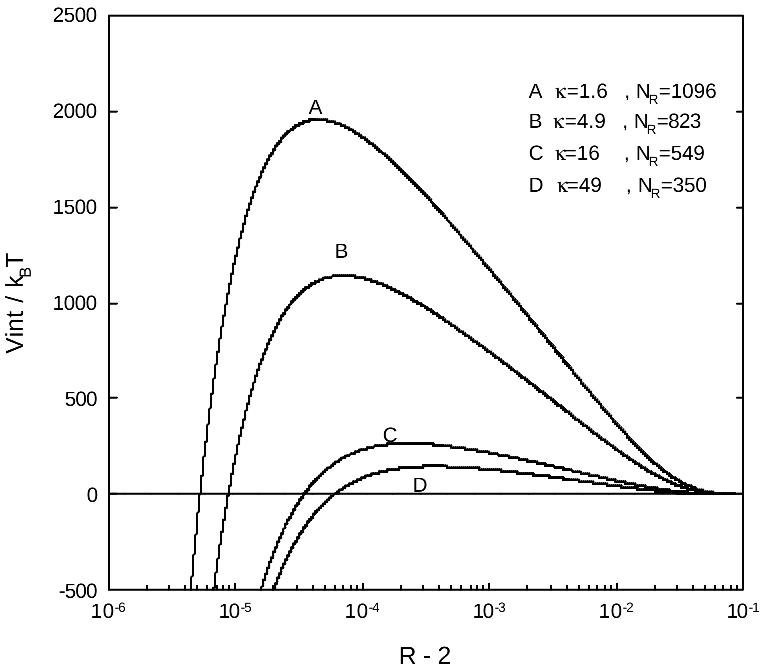

Fig[B-5] Schematic diagram of total interparticle potential energy curves for NaCl when particle diameters are at 0.807 μm and 1.1 μm, respectively。

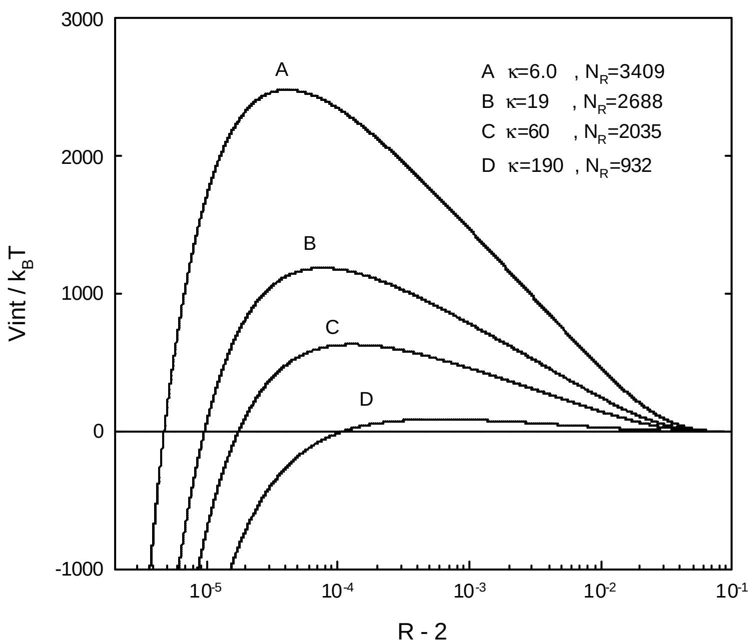

Fig[B-6] Schematic diagram of total interparticle potential energy curves for $MgCl_2$ when particle diameters are at 1.1 μm and 6.2 μm, respectively。

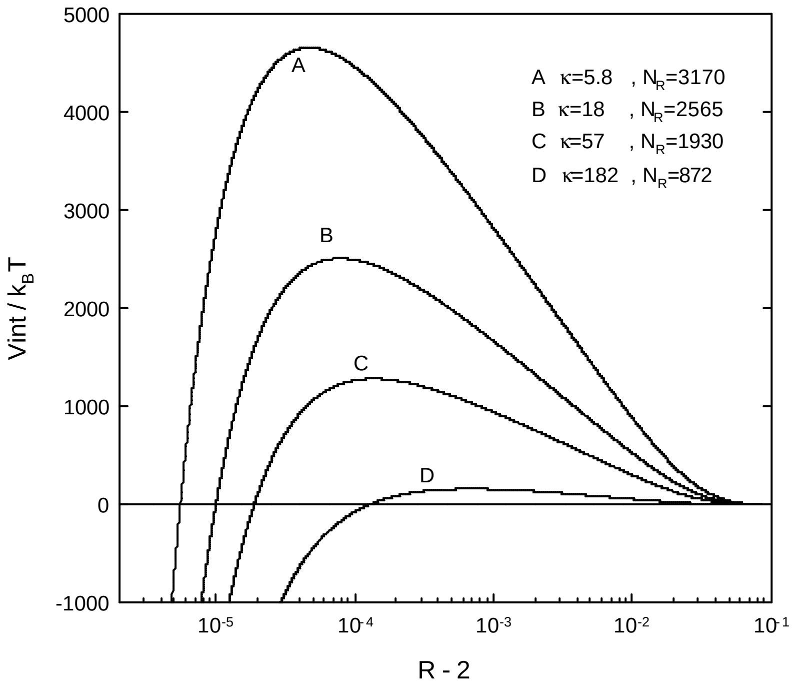

Fig[B-7] Schematic diagram of total interparticle potential energy curves for $MgCl_2$ when particle diameters are at 0.807 μm and 6.2 μm, respectively。

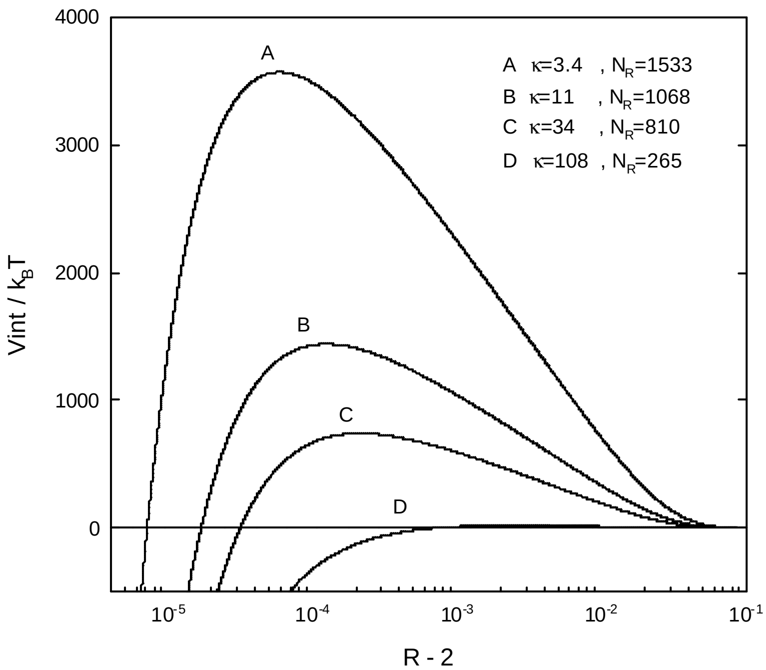

Fig[B-8] Schematic diagram of total interparticle potential energy curves for $MgCl_2$ when particle diameters are at 1.1 μm and 3.04 μm, respectively。

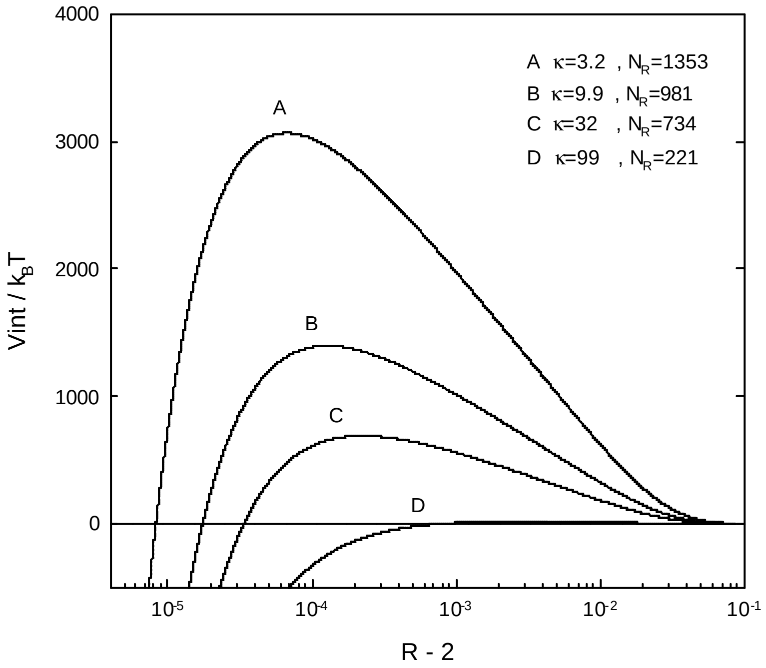

Fig[B-9] Schematic diagram of total interparticle potential energy curves for $MgCl_2$ when particle diameters are at 0.807 μm and 3.04 μm, respectively。

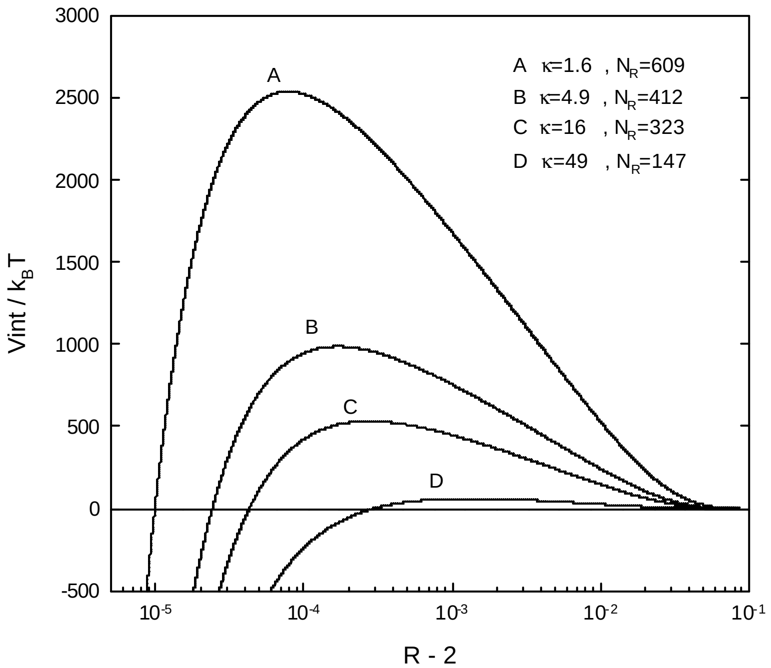

Fig[B-10] Schematic diagram of total interparticle potential energy curves for $MgCl_2$ when particle diameters are at 0.807 μm and 1.1 μm, respectively。

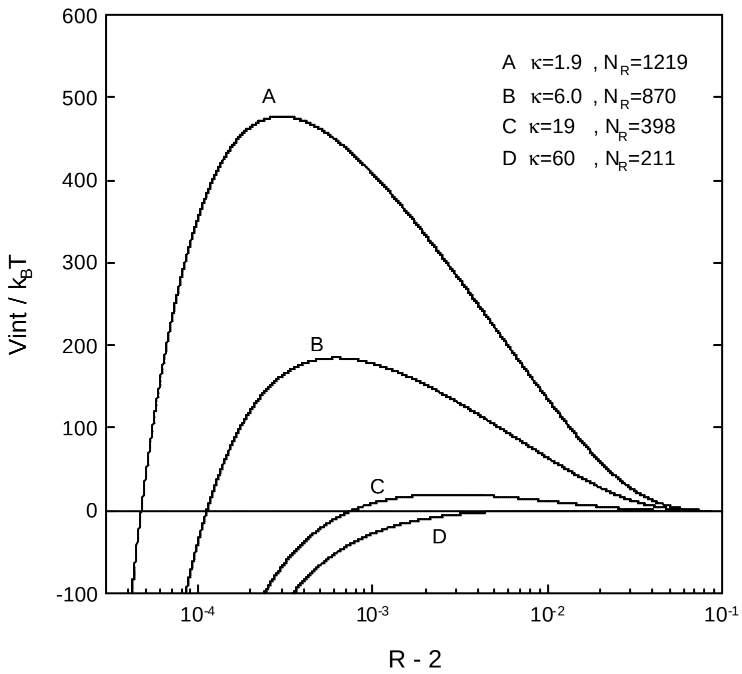

Fig[B-11] Schematic diagram of total interparticle potential energy curves for $AlCl_3$ when particle diameters are at 1.1 μm and 6.2 μm, respectively。

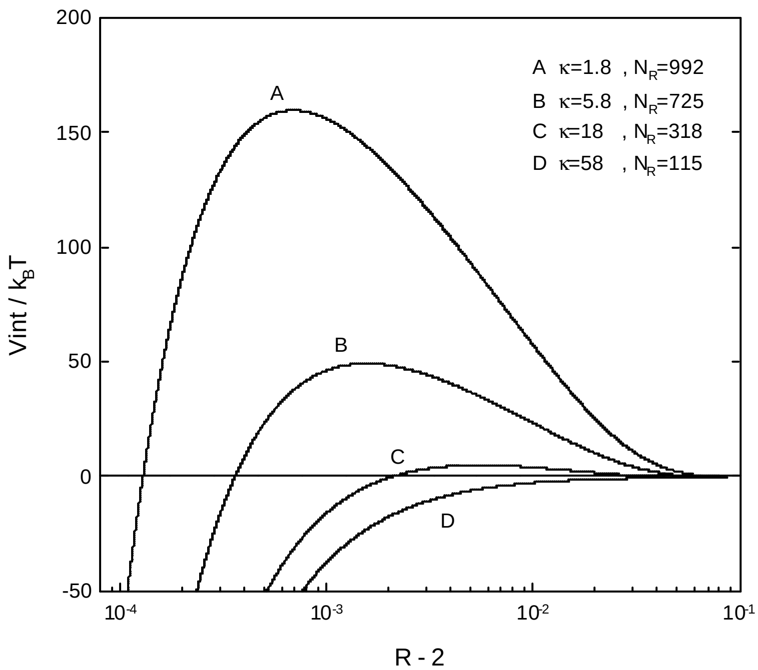

Fig[B-12] Schematic diagram of total interparticle potential energy curves for $AlCl_3$ when particle diameters are at 0.807 μm and 6.2 μm, respectively。

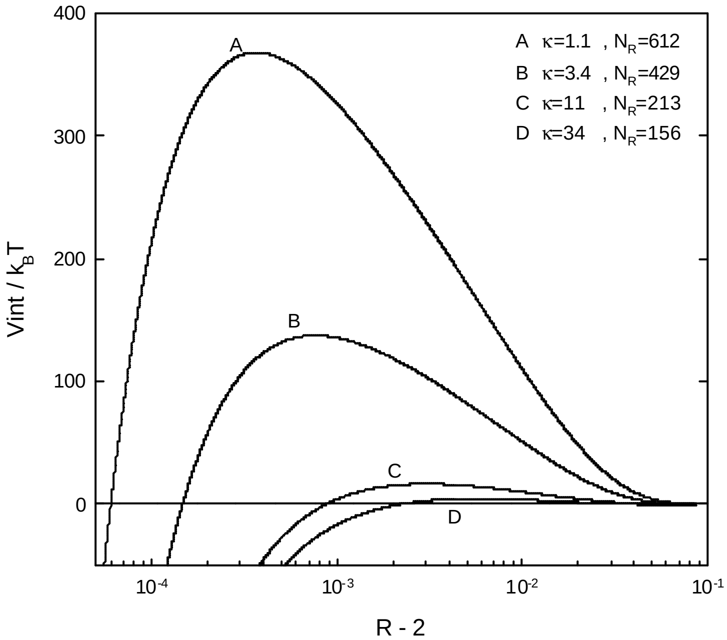

Fig[B-13] Schematic diagram of total interparticle potential energy curves for $AlCl_3$ when particle diameters are at 1.1 μm and 3.04 μm, respectively。

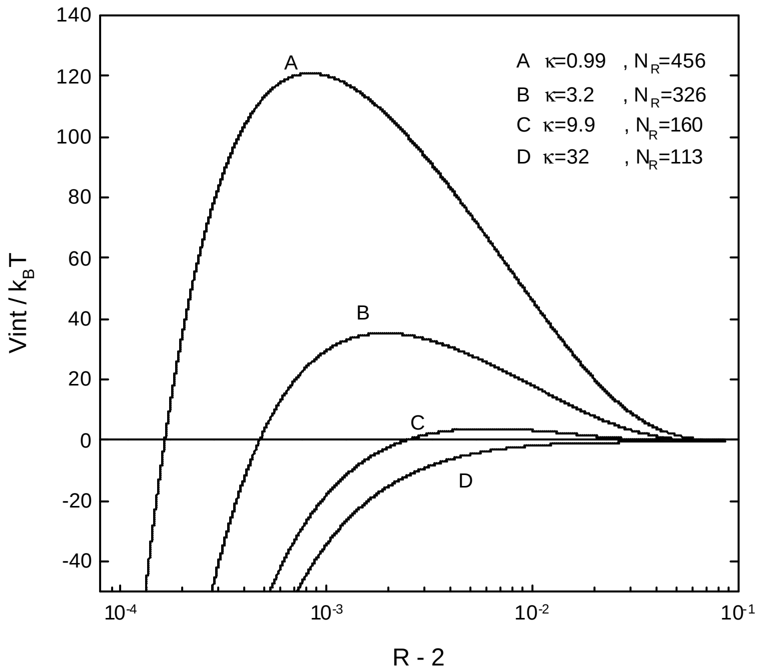

Fig[B-14] Schematic diagram of total interparticle potential energy curves for $AlCl_3$ when particle diameters are at 0.807 μm and 3.04 μm, respectively。

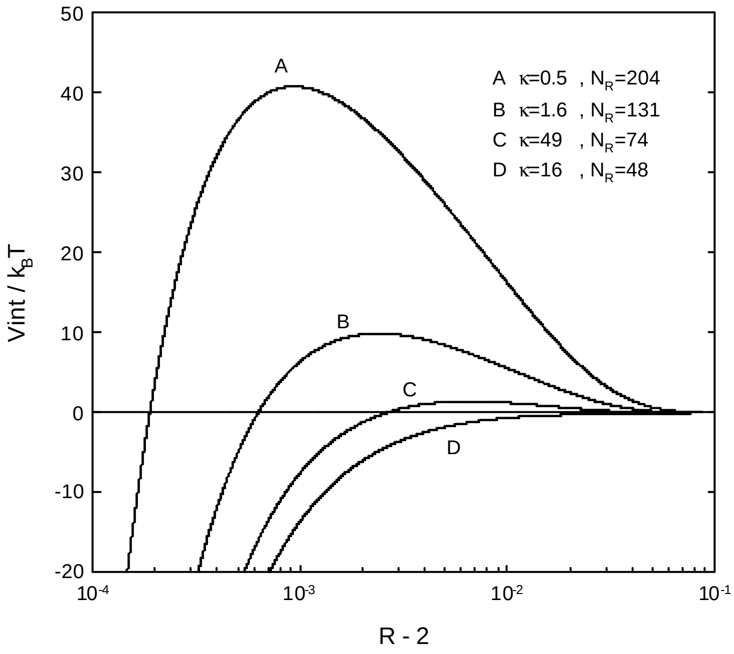

Fig[B-15] Schematic diagram of total interparticle potential energy curves for $AlCl_3$ when particle diameters are at 0.807 μm and 1.1 μm, respectively。

附錄 C

單一粒徑膠體粒子之膠凝穩定圖

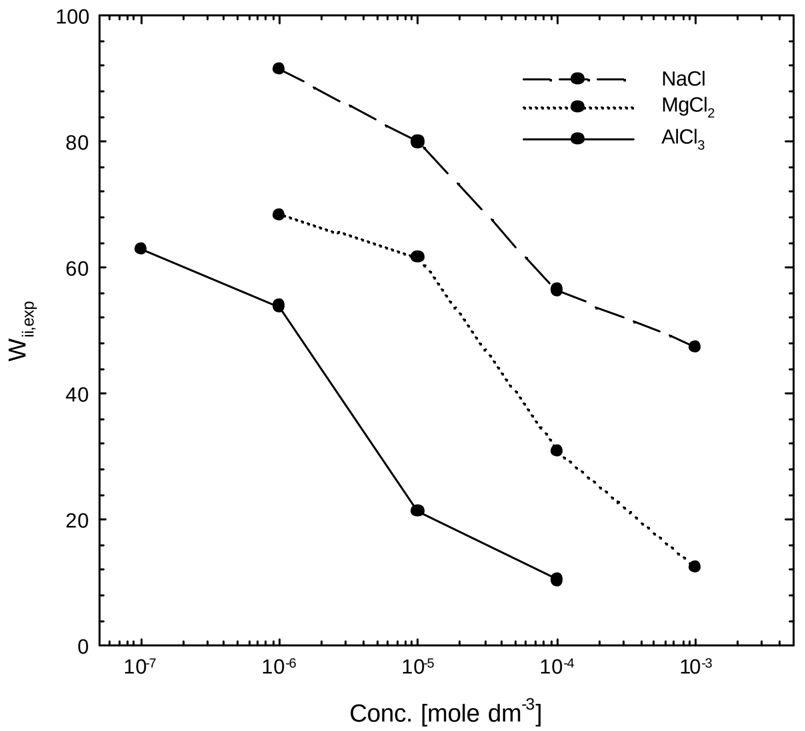

Fig[C-1] Expermiental vaules of the stability factor (W_{ii}) for 1.1 ㎛ colloids at different NaCl,$MgCl_2$,$AlCl_3$ concentrations, when G-force=1.0G

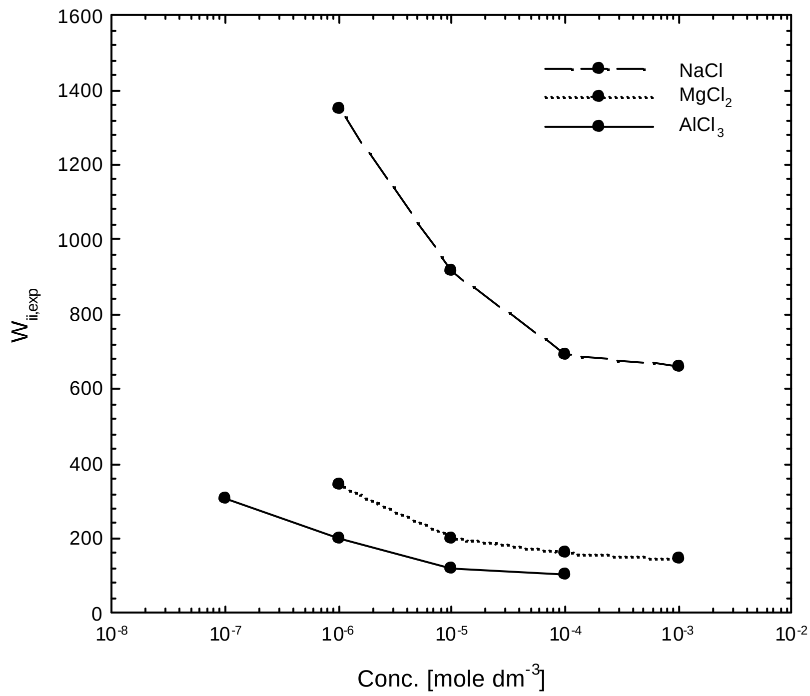

Fig[C-2] Expermiental vaules of the stability factor (W_{ii}) for 0.807 ㎛ colloids at different NaCl,$MgCl_2$, $AlCl_3$ concentrations, when G-force=1.0G

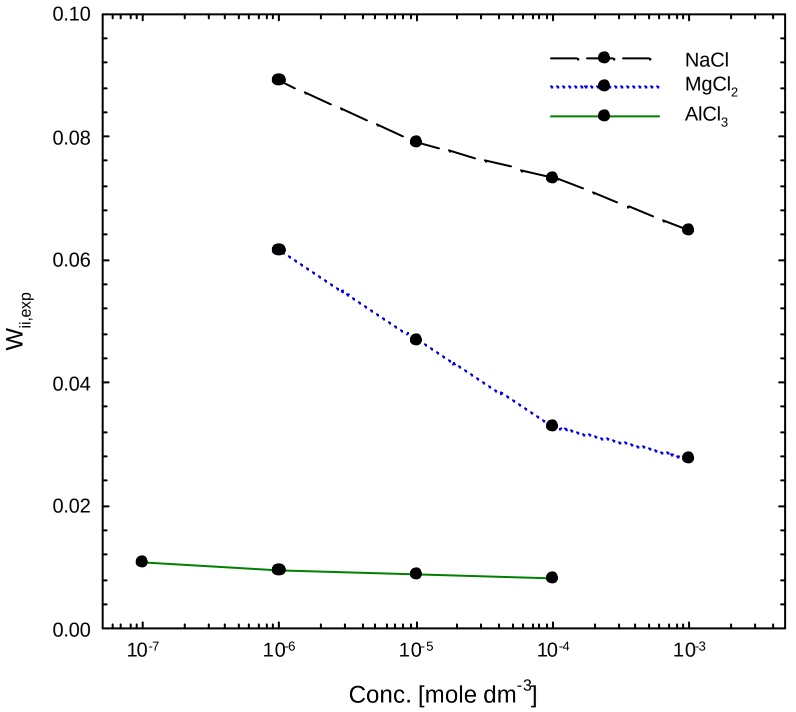

Fig[C-3] Expermiental vaules of the stability factor (W_{ii}) for 6.2㎛ colloids at different NaCl,$MgCl_2$,$AlCl_3$ concentrations, when G-force=1.5G

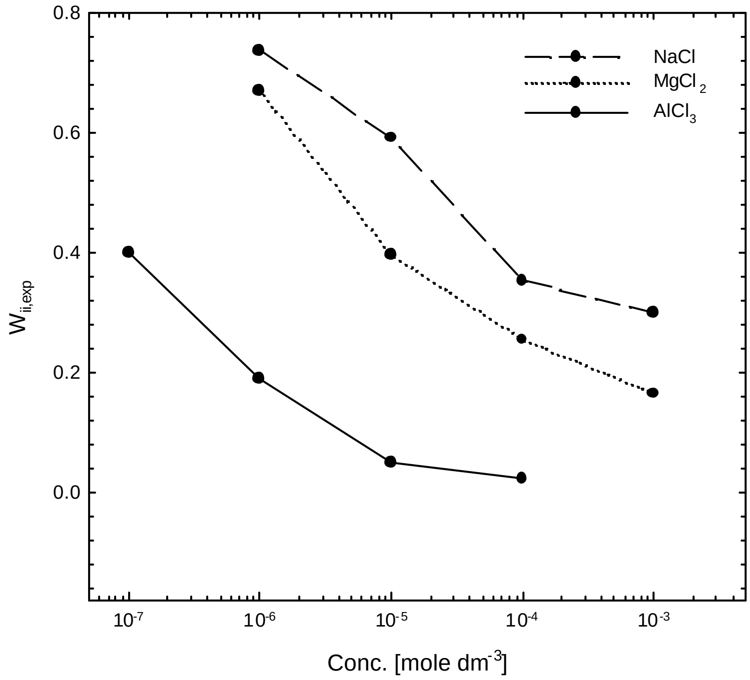

Fig[C-4] Expermiental vaules of the stability factor (W_{ii}) for 3.04㎛ colloids at different NaCl,$MgCl_2$,$AlCl_3$ concentrations, when G-force=1.5G

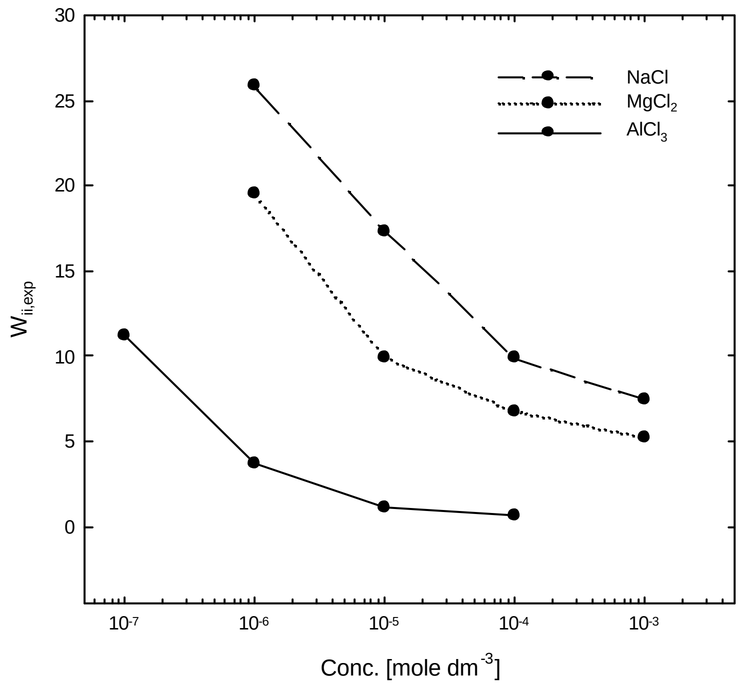

Fig[C-5] Expermiental vaules of the stability factor (W_{ii}) for 1.1㎛m colloids at different NaCl,$MgCl_2$,$AlCl_3$ concentrations, when G-force=1.5G

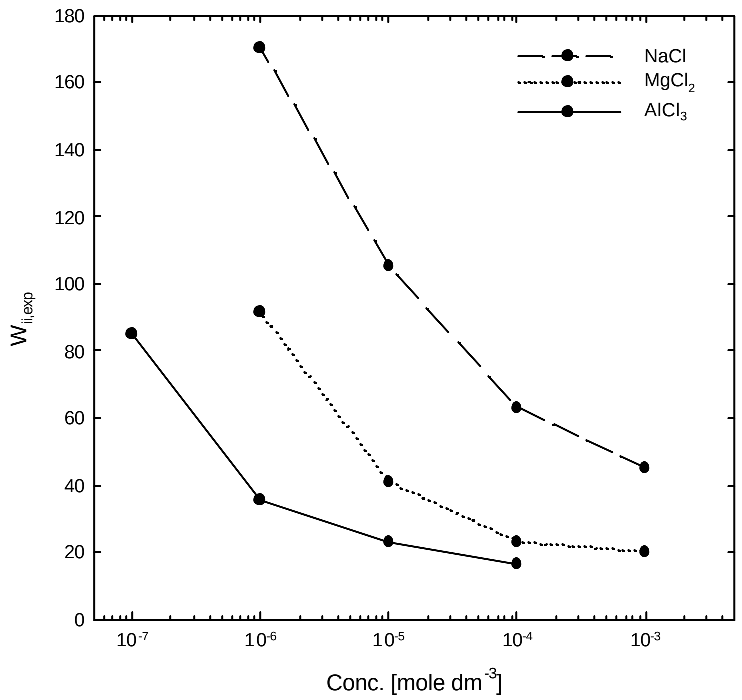

Fig[C-6] Expermiental vaules of the stability factor (W_{ii}) for 0.807㎛m colloids at different NaCl,$MgCl_2$, $AlCl_3$ concentrations, when G-force=1.5G

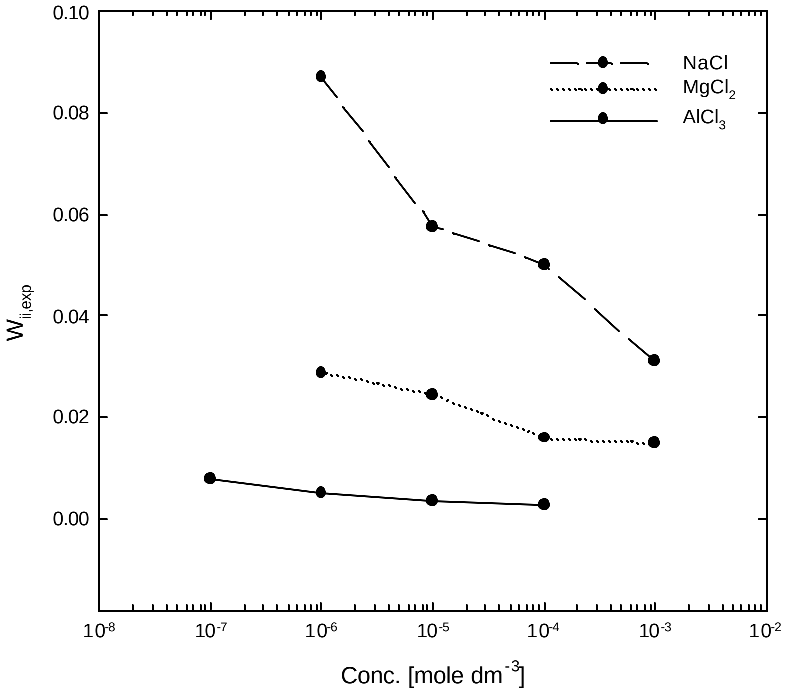

Fig[C-7] Expermiental vaules of the stability factor (W_{ii}) for 6.2㎜m colloids at different NaCl,$MgCl_2$,$AlCl_3$ concentrations, when G-force=2.0G

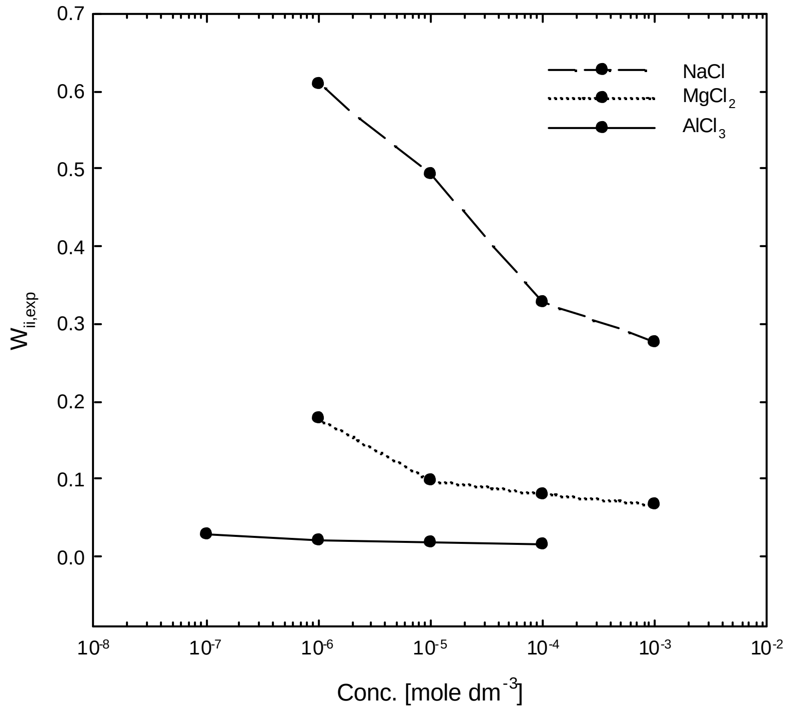

Fig[C-8] Expermiental vaules of the stability factor (W_{ii}) for 3.04㎜m colloids at different NaCl,$MgCl_2$,$AlCl_3$ concentrations, when G-force=2.0G

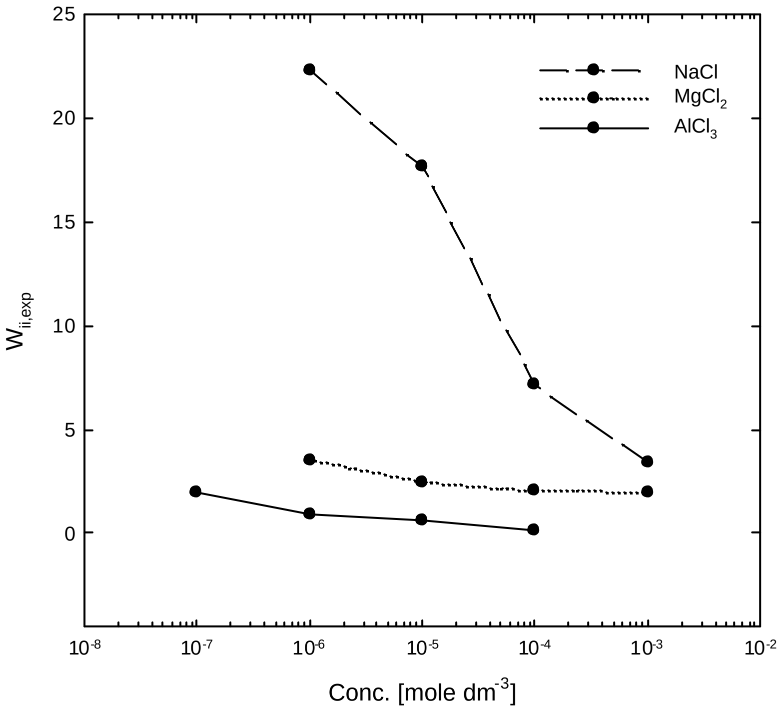

Fig[C-9] Expermiental vaules of the stability factor (W_{ii}) for 1.1㎛ colloids at different NaCl,$MgCl_2$,$AlCl_3$ concentrations, when G-force=2.0G

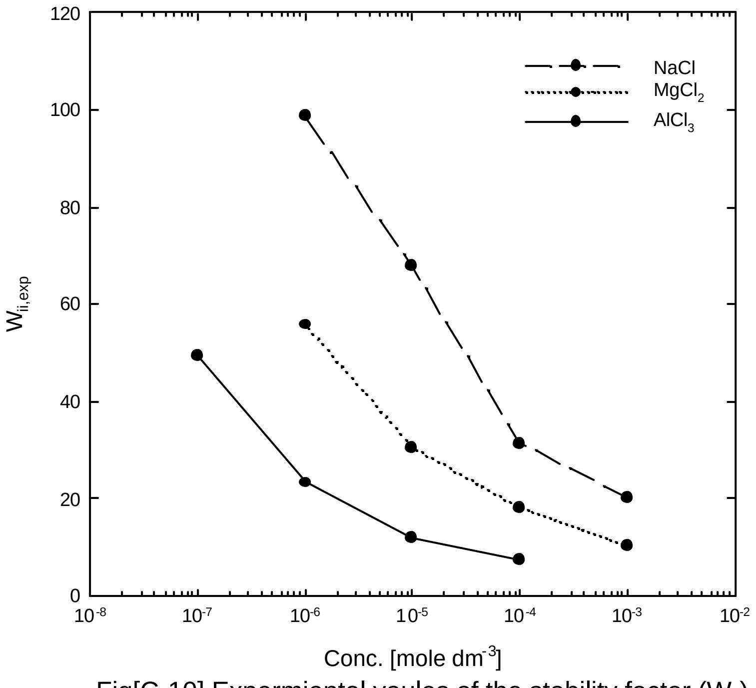

Fig[C-10] Expermiental vaules of the stability factor (W_{ii}) for 0.807㎛ colloids at different NaCl,$MgCl_2$, $AlCl_3$ concentrations, when G-force=2.0G

附錄 D

不同粒徑膠體粒子等濃度混合之膠凝穩定圖

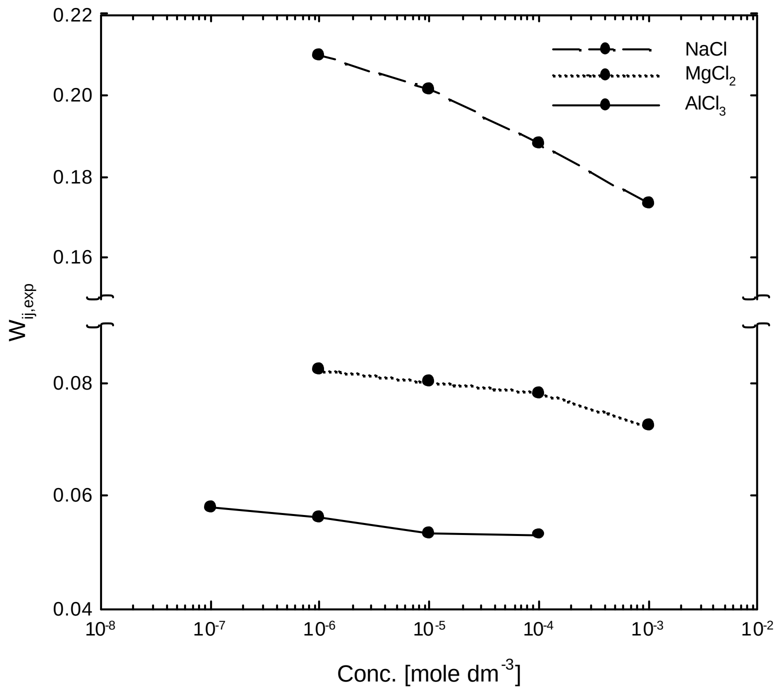

Fig[D-1] Expermiental vaules of the stability factor (W_{ij}) for 6.2 ㎜m and 1.1 ㎜m colloids at different NaCl,$MgCl_2$, $AlCl_3$ concentrations, when G-force=1.0G

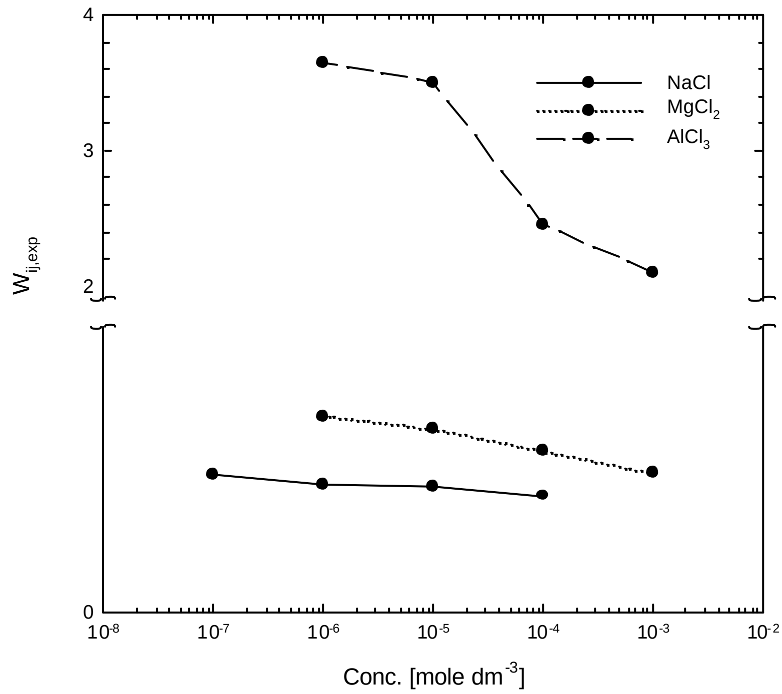

Fig[D-2] Expermiental vaules of the stability factor (W_{ij}) for 6.2 ㎜m and 0.807 ㎜m colloids at different NaCl , $MgCl_2$,$AlCl_3$ concentrations, when G-force=1.0G

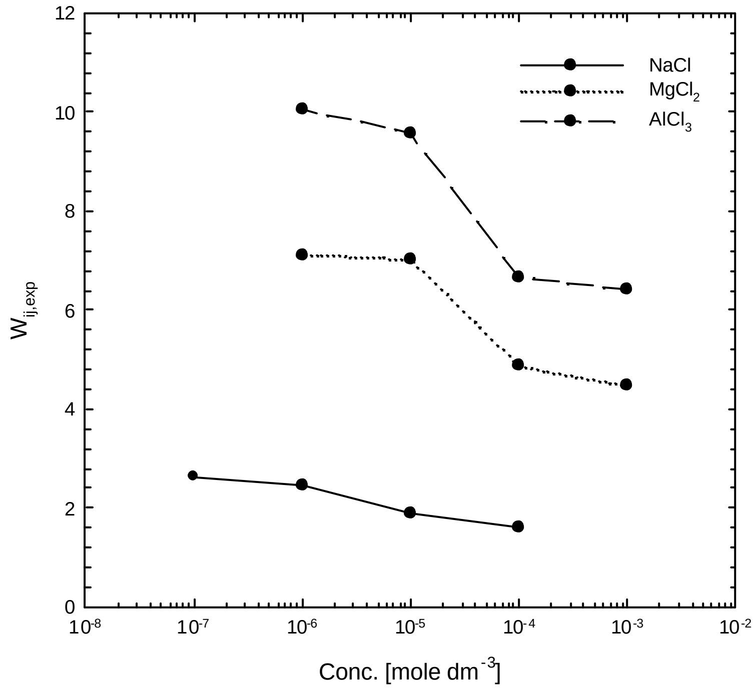

Fig[D-3] Expermiental vaules of the stability factor (W_{ij}) for 3.04 ㎛m and 1.1 ㎛m colloids at different NaCl , $MgCl_2$,$AlCl_3$ concentrations, when G-force=1.0G

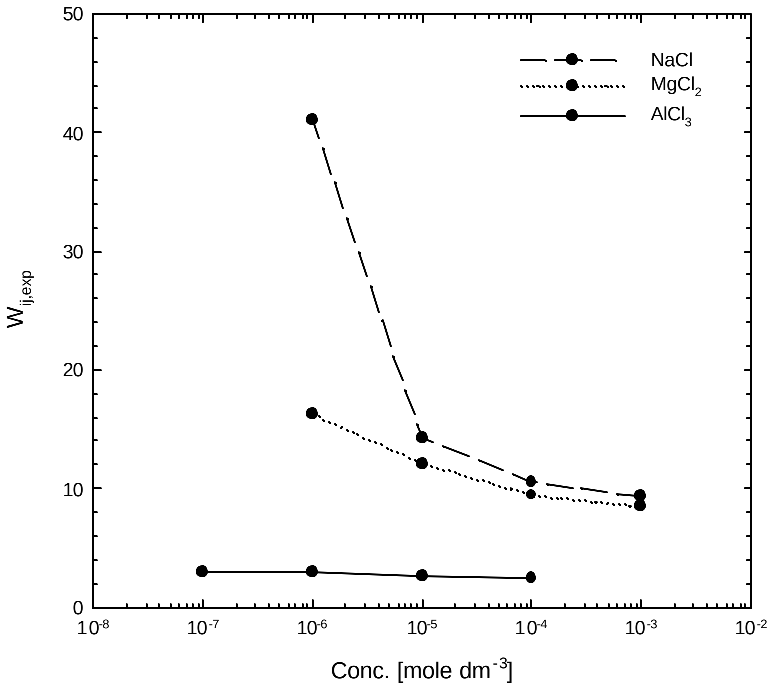

Fig[D-4] Expermiental vaules of the stability factor (W_{ij}) for 3.04 ㎛m and 0.807 ㎛m colloids at different NaCl , $MgCl_2$,$AlCl_3$ concentrations, when G-force=1.0G

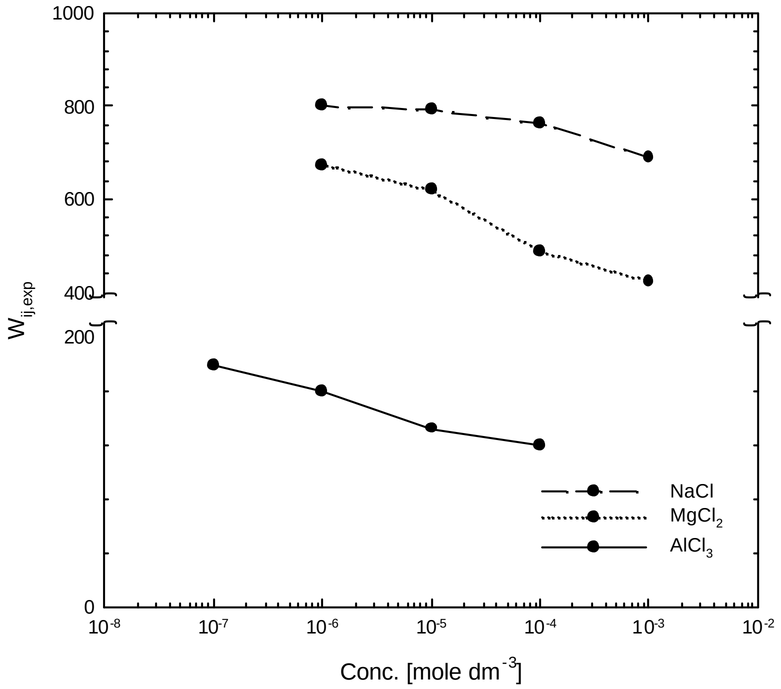

Fig[D-5] Expermiental vaules of the stability factor (W_{ij}) for 1.1 ㎜ and 0.807 ㎜ colloids at different NaCl , $MgCl_2$,$AlCl_3$ concentrations, when G-force=1.0G

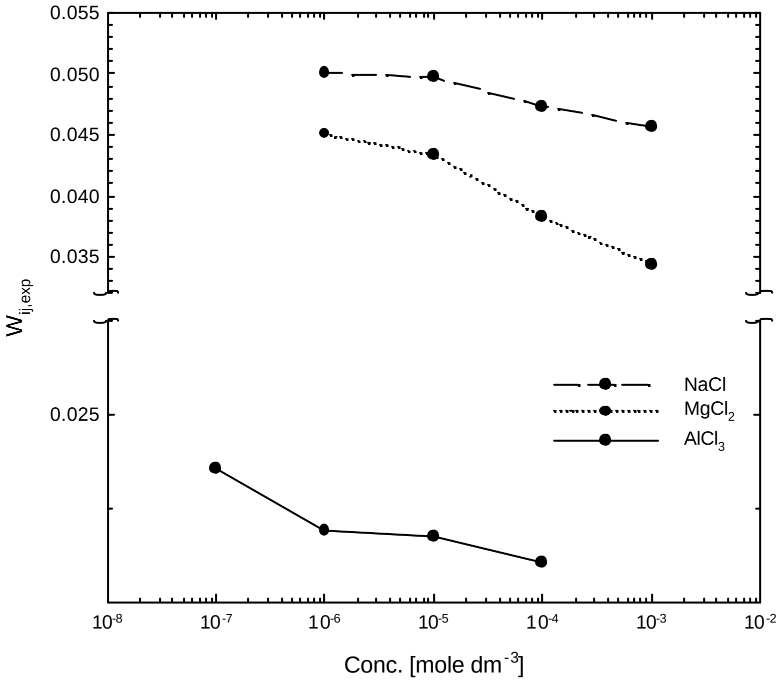

Fig[D-6] Expermiental vaules of the stability factor (W_{ij}) for 6.2 ㎜ and 3.04 ㎜ colloids at different NaCl , $MgCl_2$,$AlCl_3$ concentrations, when G-force=1.5G

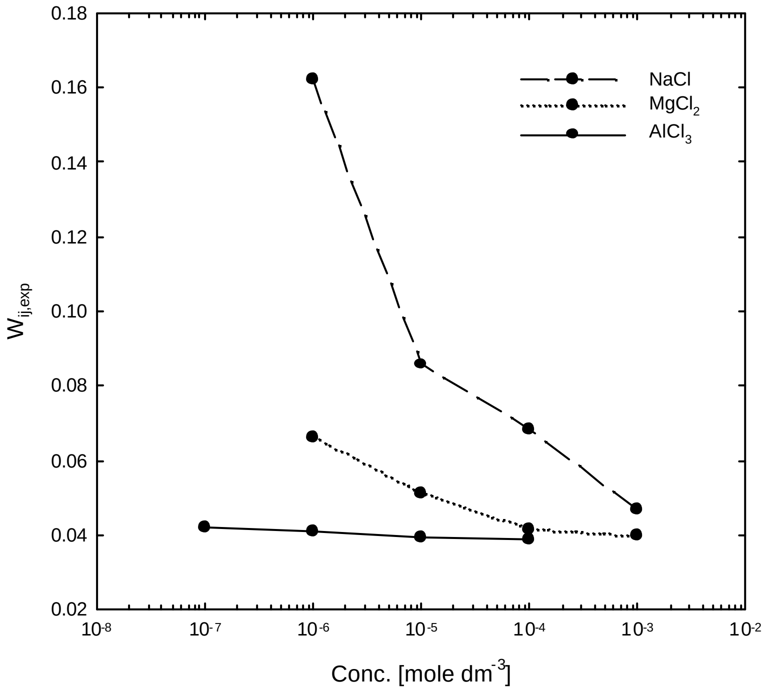

Fig[D-7] Expermiental vaules of the stability factor (W_{ij}) for 6.2 ㎛ and 1.1 ㎛ colloids at different NaCl , $MgCl_2$,$AlCl_3$ concentrations, when G-force=1.5G

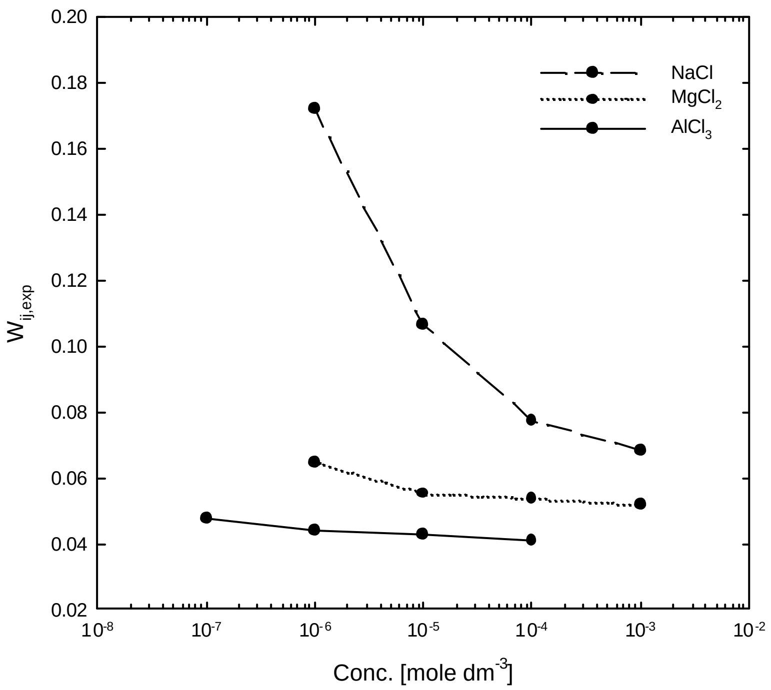

Fig[D-8] Expermiental vaules of the stability factor (W_{ij}) for 6.2 ㎛ and 0.807 ㎛ colloids at different NaCl , $MgCl_2$,$AlCl_3$ concentrations, when G-force=1.5G

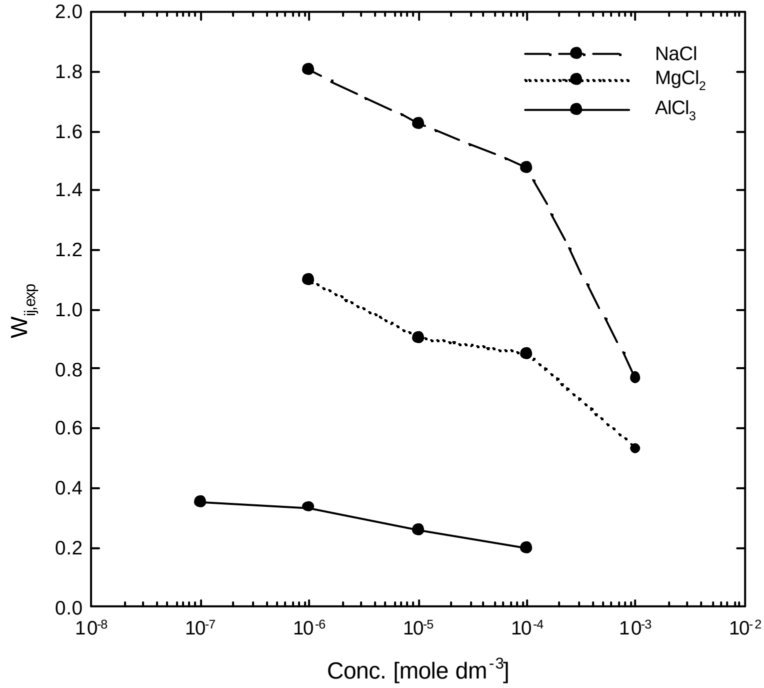

Fig[D-9] Expermiental vaules of the stability factor (W_{ij}) for 3.04 ㎜ and 1.1 ㎜ colloids at different NaCl , $MgCl_2$,$AlCl_3$ concentrations, when G-force=1.5G

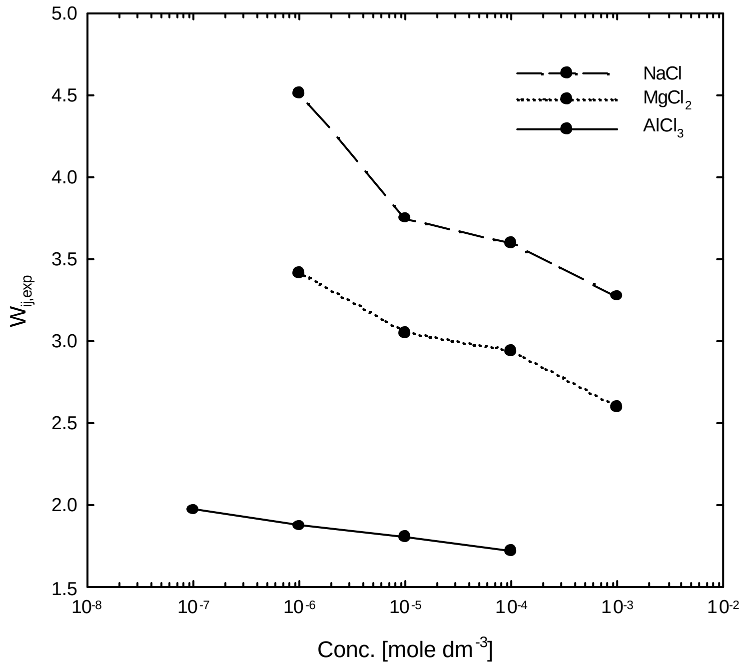

Fig[D-10] Expermiental vaules of the stability factor (W_{ij}) for 3.04 ㎜ and 0.807 ㎜ colloids at different NaCl , $MgCl_2$,$AlCl_3$ concentrations, when G-force=1.5G

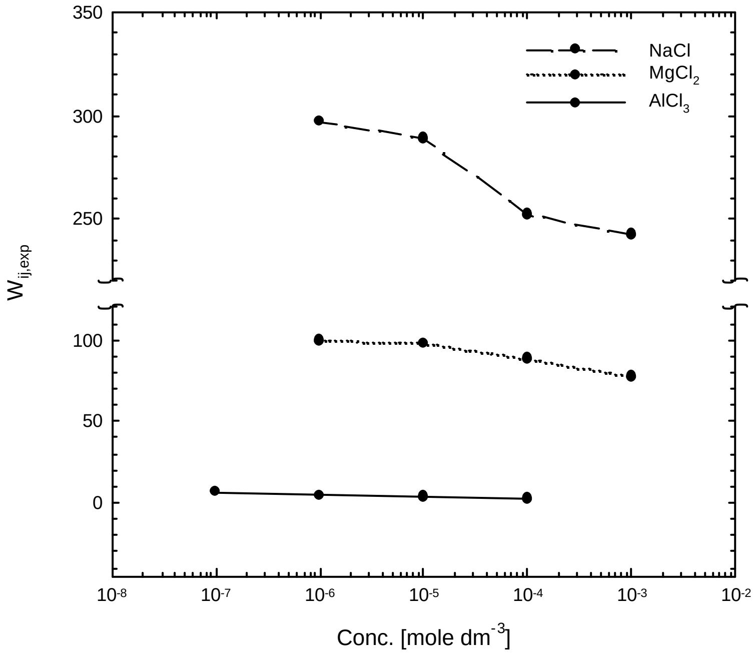

Fig[D-11] Expermiental vaules of the stability factor (W_{ij}) for 1.1 ㎜m and 0.807 ㎜m colloids at different NaCl , $MgCl_2$,$AlCl_3$ concentrations, when G-force=1.5G

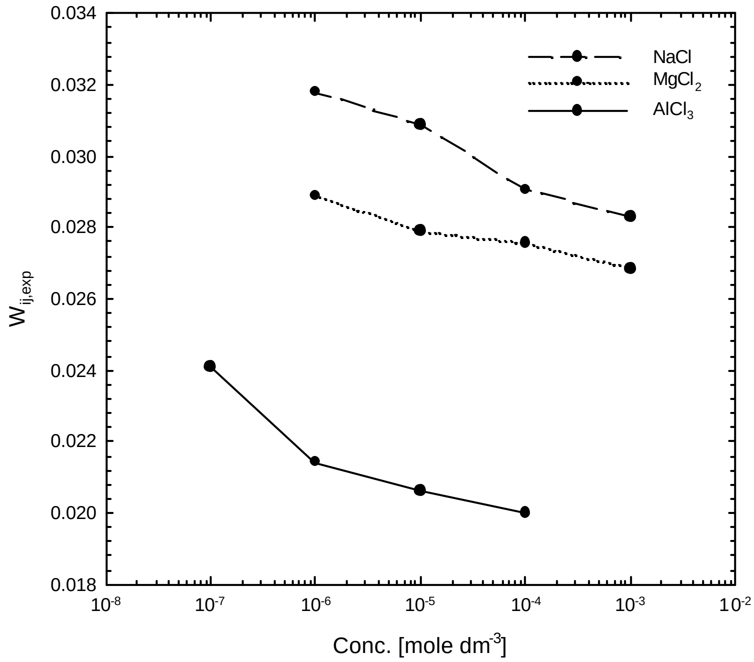

Fig[D-12] Expermiental vaules of the stability factor (W_{ij}) for 6.2 ㎜m and 3.04 ㎜m colloids at different NaCl , $MgCl_2$,$AlCl_3$ concentrations, when G-force=2.0G

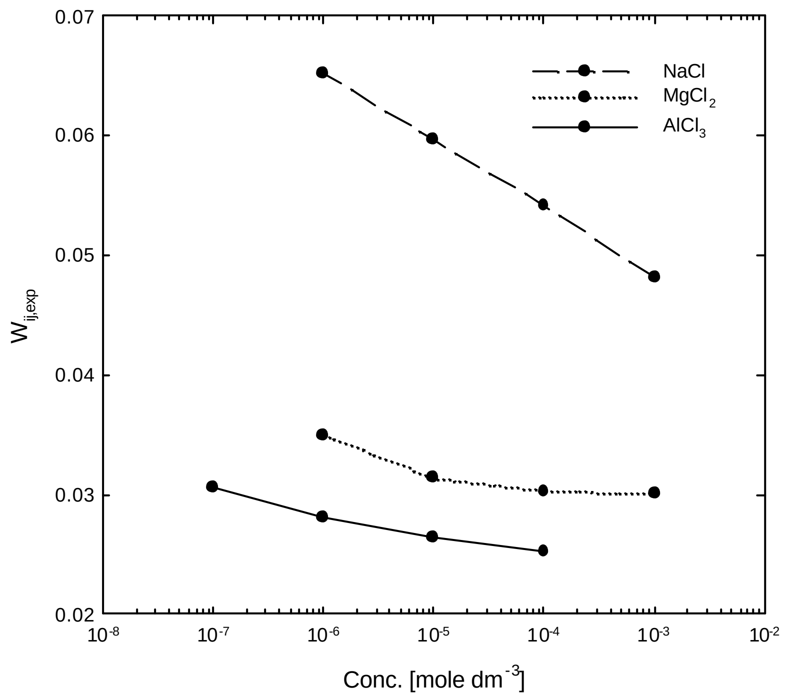

Fig[D-13] Expermiental vaules of the stability factor (W_{ij}) for 6.2 ㎜ and 1.1 ㎜ colloids at different NaCl , $MgCl_2$,$AlCl_3$ concentrations, when G-force=2.0G

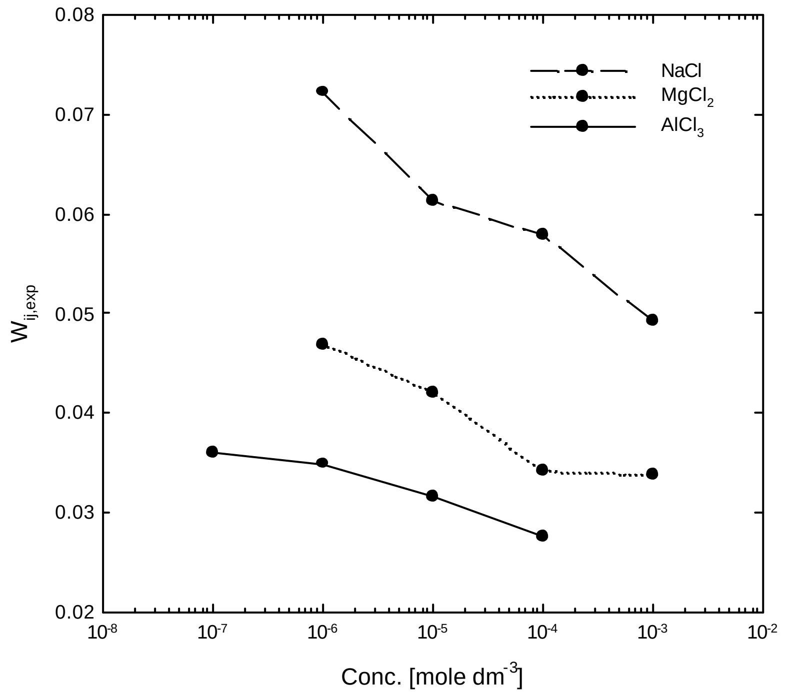

Fig[D-14] Expermiental vaules of the stability factor (W_{ij}) for 6.2 ㎜ and 0.807㎜ colloids at different NaCl , $MgCl_2$,$AlCl_3$ concentrations, when G-force=2.0G

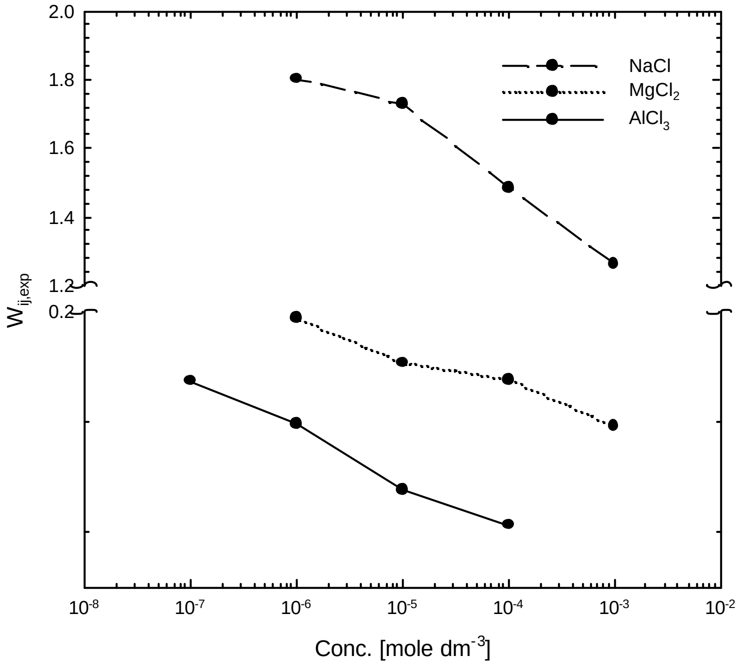

Fig[D-15] Expermiental vaules of the stability factor (W_{ij}) for 3.04 ㎜m and 1.1 ㎜m colloids at different NaCl , $MgCl_2$,$AlCl_3$ concentrations, when G-force=2.0G

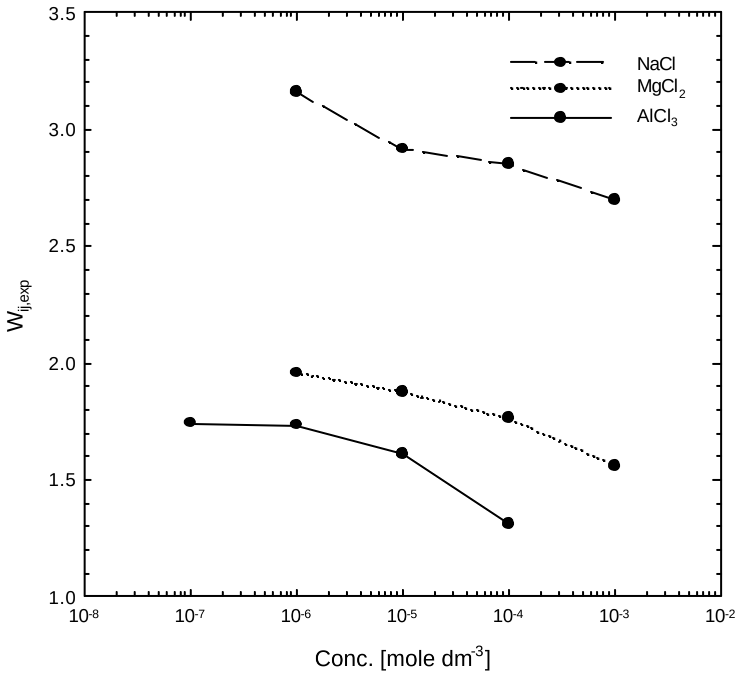

Fig[D-16] Expermiental vaules of the stability factor (W_{ij}) for 3.04 ㎜m and 0.807 ㎜m colloids at different NaCl , $MgCl_2$,$AlCl_3$ concentrations, when G-force=2.0G

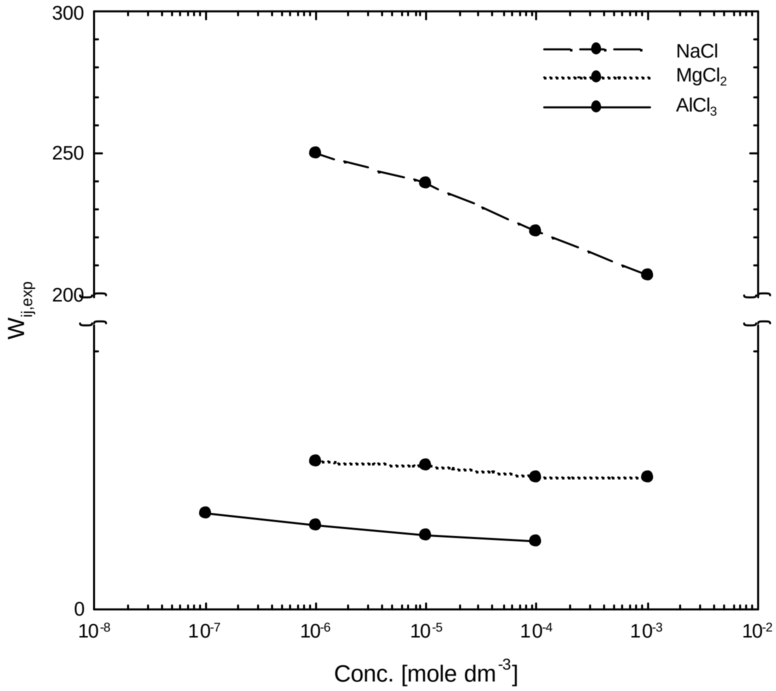

Fig[D-17] Expermiental vaules of the stability factor (W_{ij}) for 1.1 ㎜ and 0.807 ㎜ colloids at different NaCl , $MgCl_2$,$AlCl_3$ concentrations, when G-force=2.0G

附錄 E

不同粒徑膠體粒子等濃度混合膠凝沉降時在不同重力值下的 κ -N_G 圖

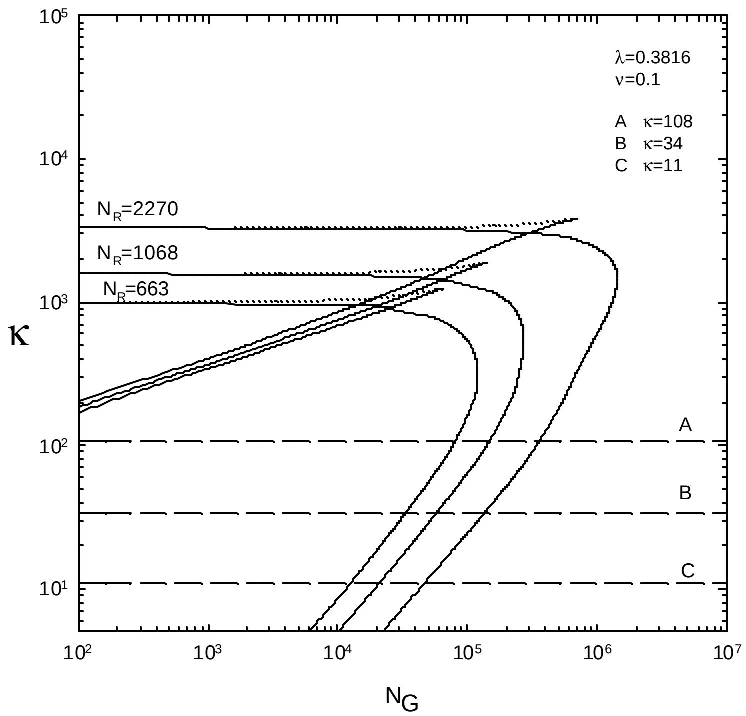

Fig[E-1] Effect of surface potential on the κ - N_G stability plane for the various electrolyte(NaCl) at particle size ratio=0.3816.

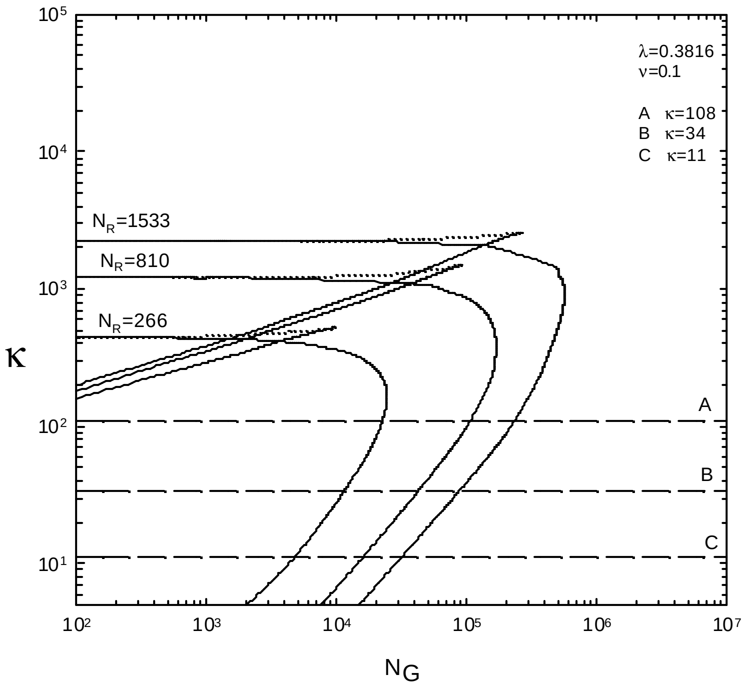

Fig[E-2] Effect of surface potential on the κ - N_G stability plane for the various electrolyte($MgCl_2$) at particle size ratio=0.3816.

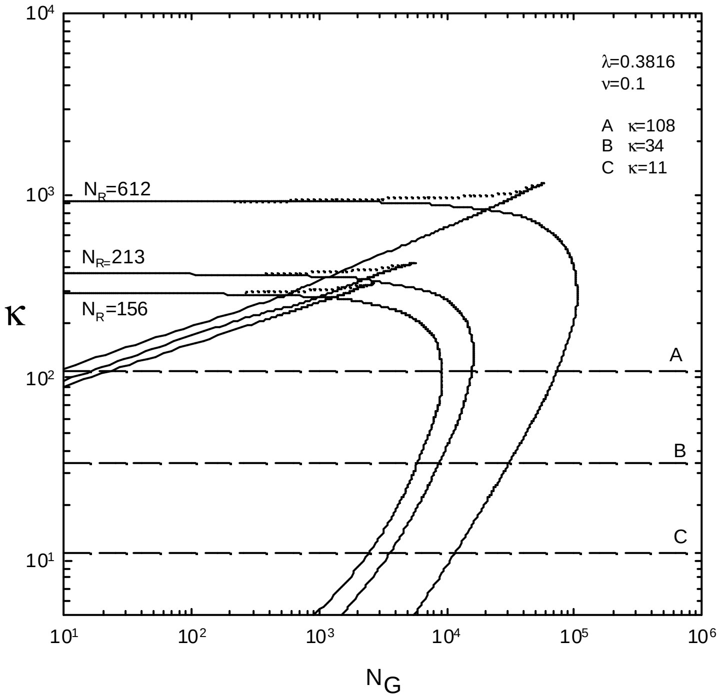

Fig[E-3] Effect of surface potential on the κ - N_G stability plane for the various electrolyte($AlCl_3$) at particle size ratio=0.3816.

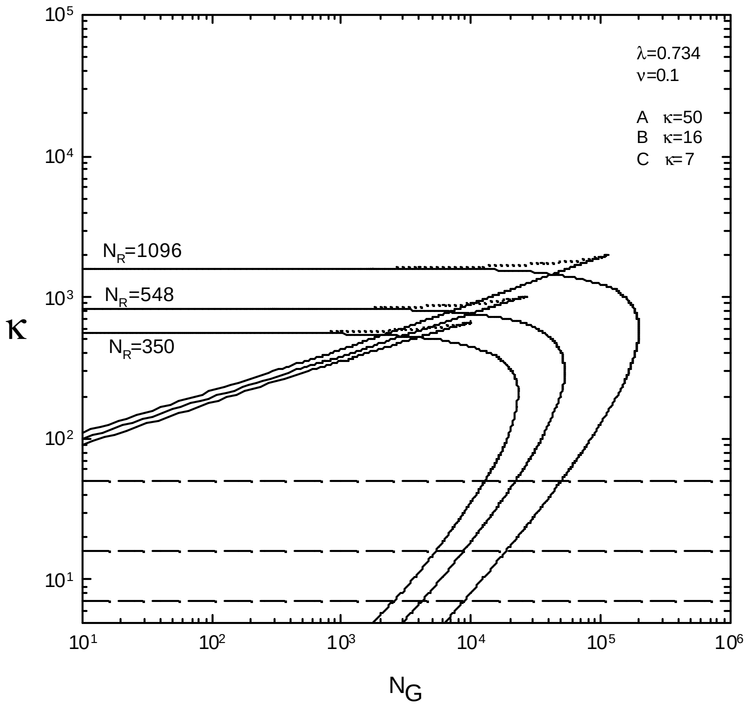

Fig[E-4] Effect of surface potential on the κ - N_G stability plane for the various electrolyte(NaCl) at particle size ratio=0.734.

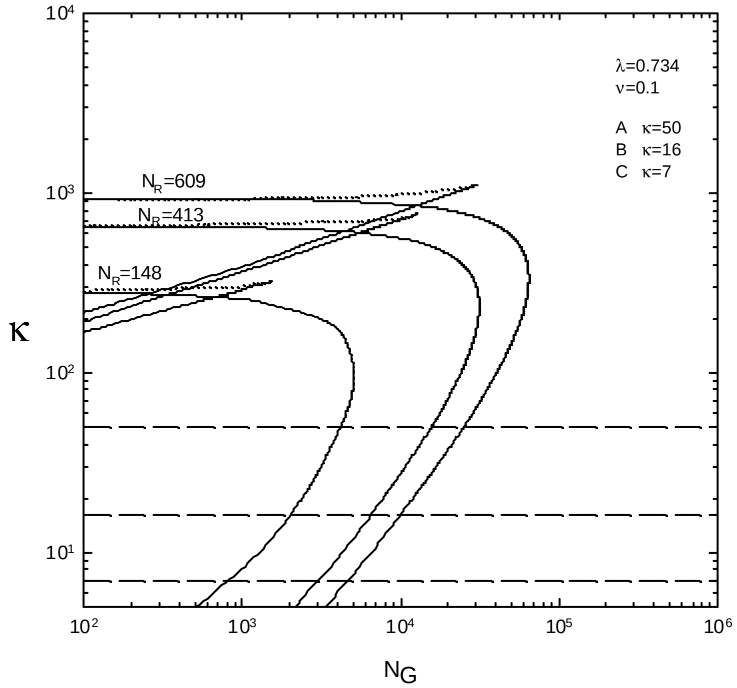

Fig[E-5] Effect of surface potential on the κ - N_G stability plane for the various electrolyte($MgCl_2$) at particle size ratio=0.734

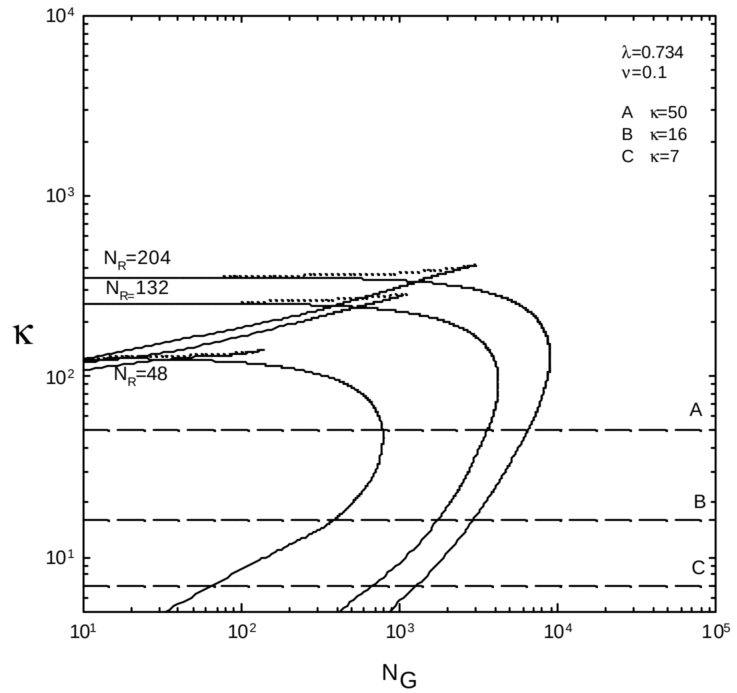

Fig[E-6] Effect of surface potential on the κ - N_G stability plane for the various electrolyte($AlCl_3$) at particle size ratio=0.734.

附錄 F

不同粒徑膠體等濃度混合膠凝沉降
之理論凝集效率

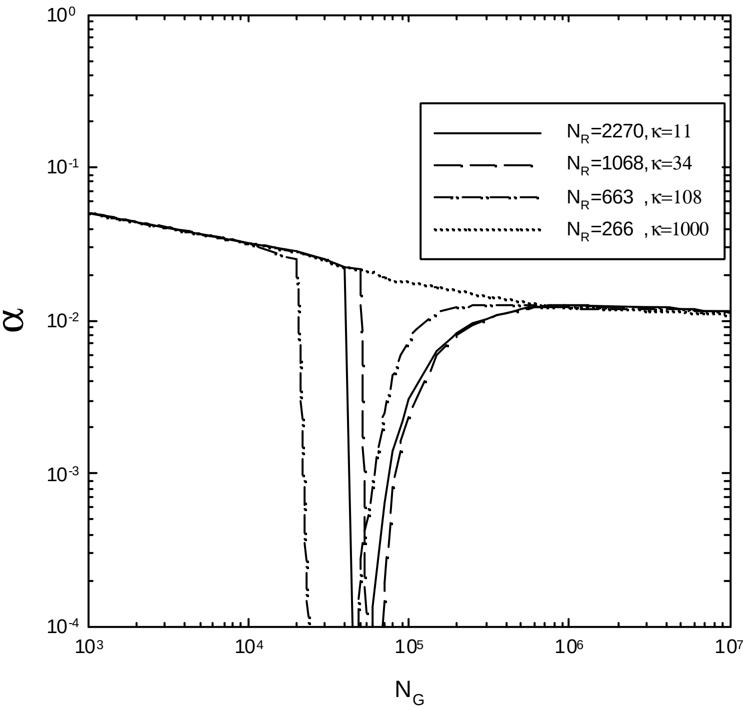

Fig[F-1] Effect of gravity on the capture efficiency for the various electrolyte (NaCl) concentration at particle size ratio=0.3816.

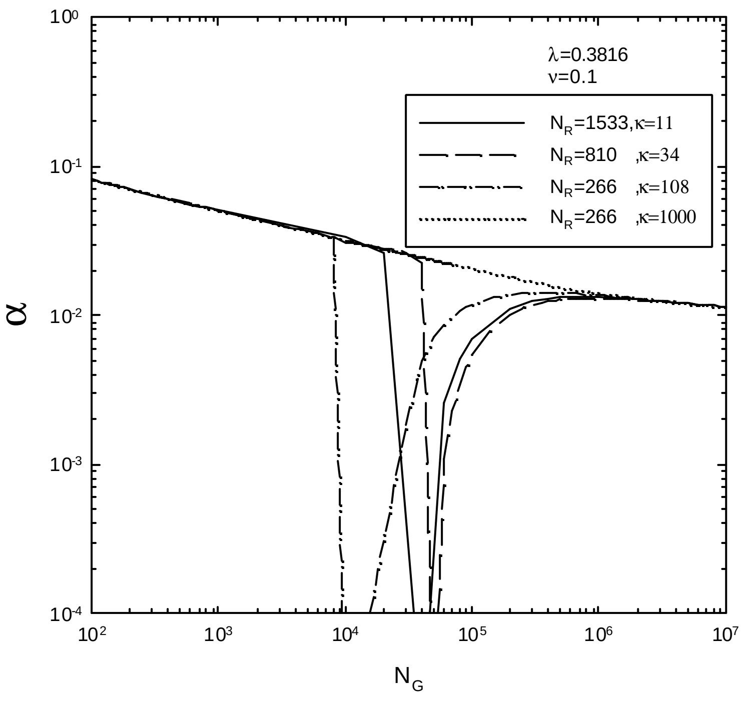

Fig[F-2] Effect of gravity on the capture efficiency for the various electrolyte ($MgCl_2$) concentration at particle size ratio=0.3816.

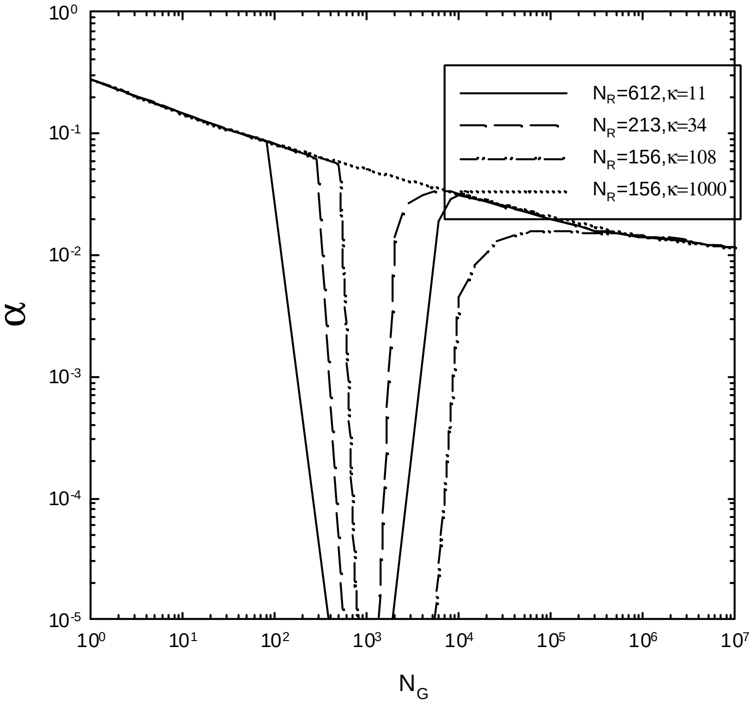

Fig[F-3] Effect of gravity on the capture efficiency for the various electrolyte ($AlCl_3$) concentration at particle size ratio=0.3816.

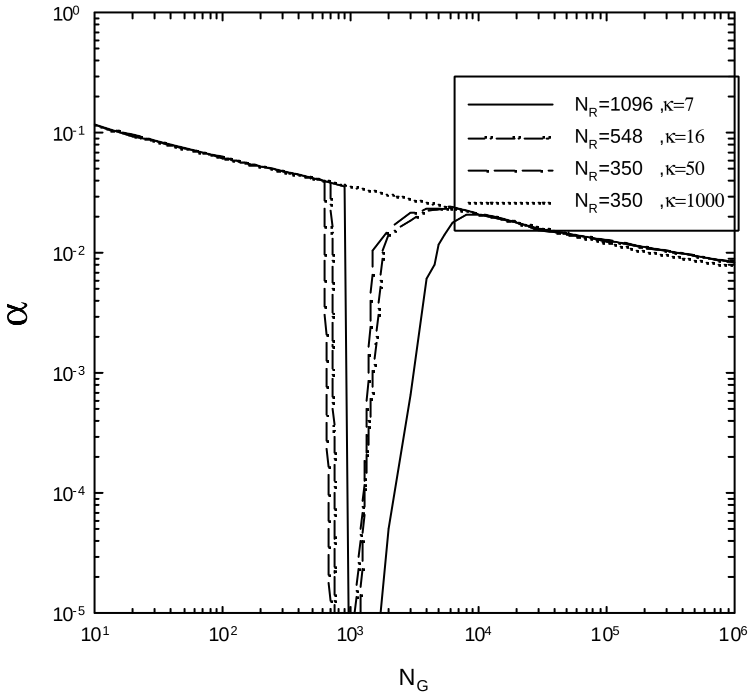

Fig[F-4] Effect of gravity on the capture efficiency for the various electrolyte (NaCl) concentration at particle size ratio=0.734.

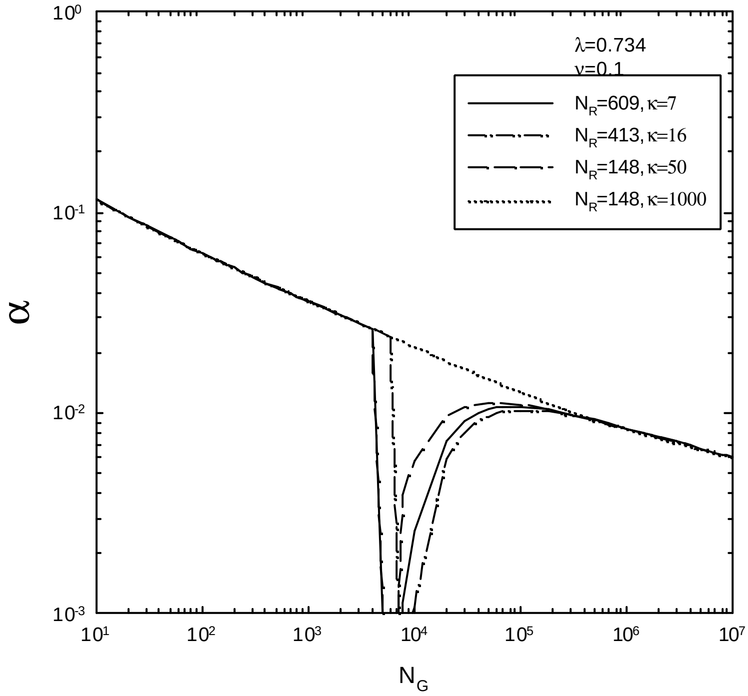

Fig[F-5] Effect of gravity on the capture efficiency for the various electrolyte ($MgCl_2$) concentration at particle size ratio=0.734.

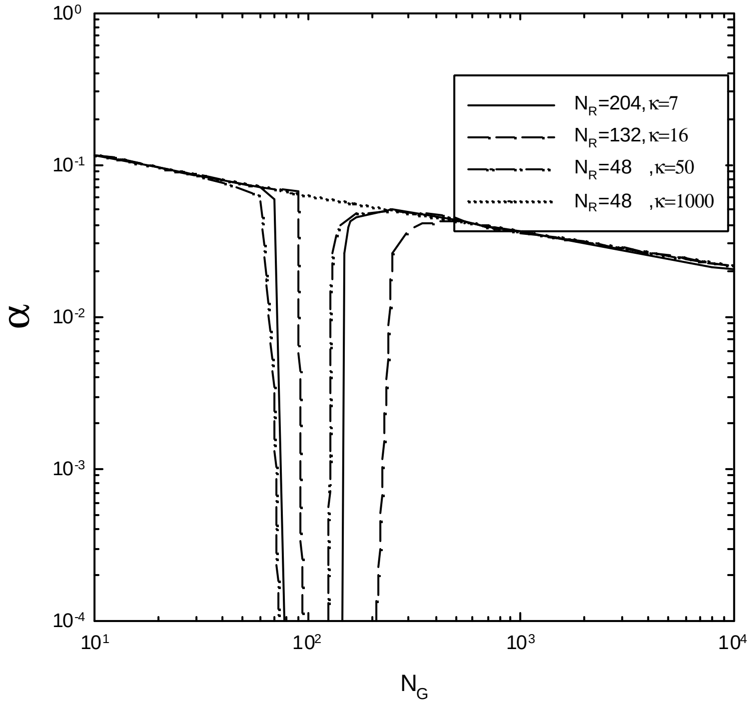

Fig[F-6] Effect of gravity on the capture efficiency for the various electrolyte ($AlCl_3$) concentration at particle size ratio=0.734.

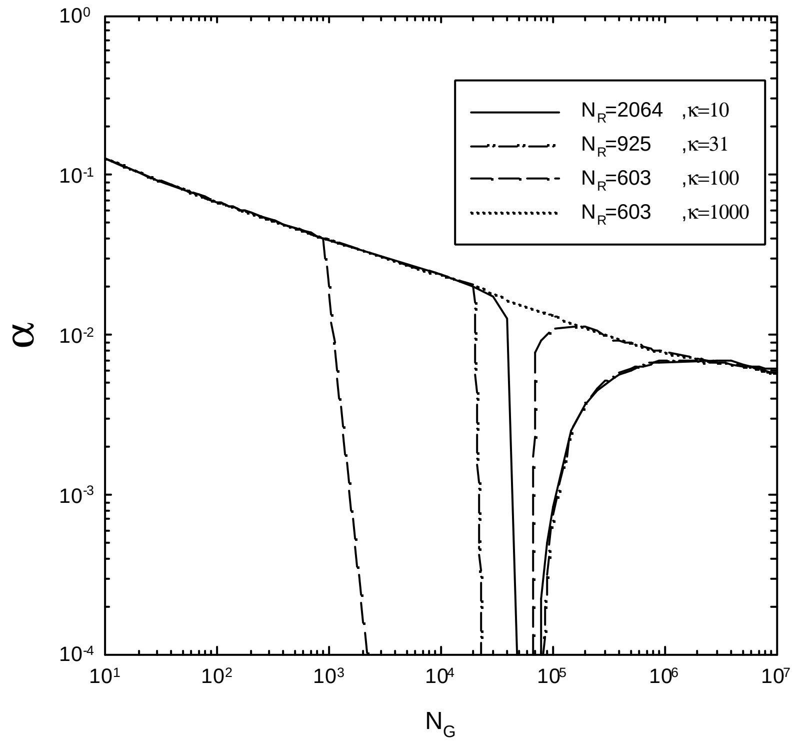

Fig[F-7] Effect of gravity on the capture efficiency for the various electrolyte (NaCl) concentration at particle size ratio=0.266.

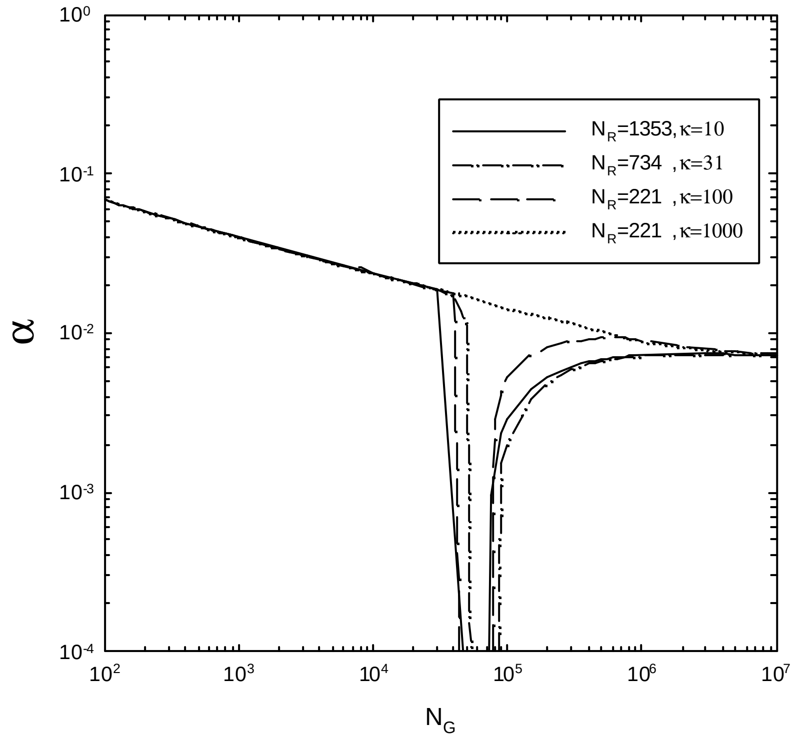

Fig[F-8] Effect of gravity on the capture efficiency for the various electrolyte ($MgCl_2$) concentration at particle size ratio=0.266.

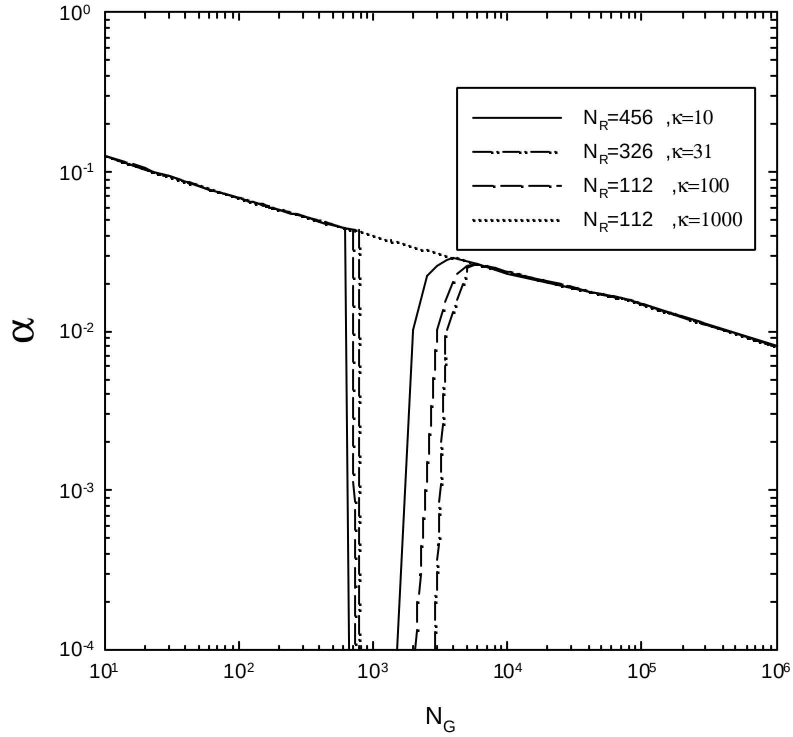

Fig[F-9] Effect of gravity on the capture efficiency for the various electrolyte ($AlCl_3$) concentration at particle size ratio=0.266.

附錄 G

其它參考資料

(一)實驗步驟之－檢量線之製作

（一）製作濁度（turbidity**）對粒子濃度的檢量線（**calibration curve**）：**

1.**由上述配製好的膠體溶液基準品各量取** 1~10ml **再分別稀釋成** 100ml。

2.**各取** 1ml **的稀釋膠體溶液加入** 49ml ISOTON **電解質，利用** coulter counter **測量膠體的粒子濃度。**

3.**由** 1.**的膠體稀釋溶液取** 15ml **量測其初始（**initial**）濁度值。**

4.**由** 2.**和** 3.**可得出濁度對膠體粒子濃度的關係，並方便未來做等濃度不同膠體粒子間的混和沉降實驗。**

(二) V_{total}、W_{ii}、W_{ij}和 W_{mix} 計算之流程圖：

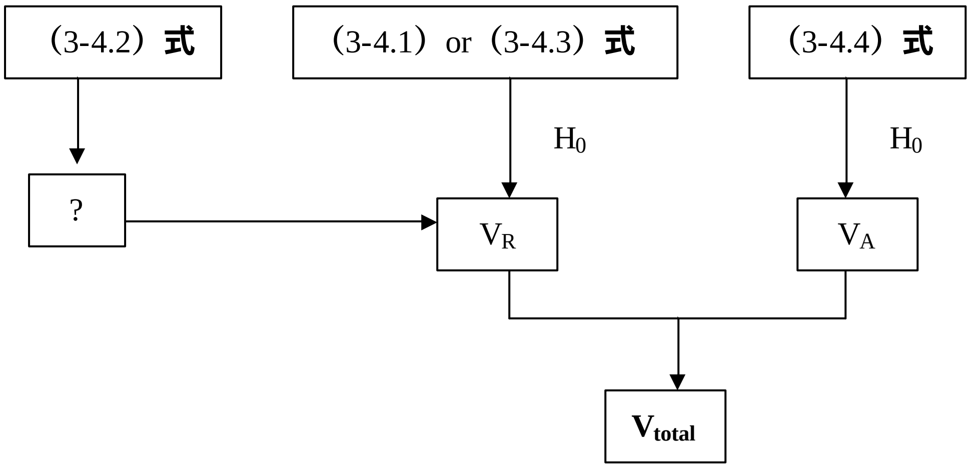

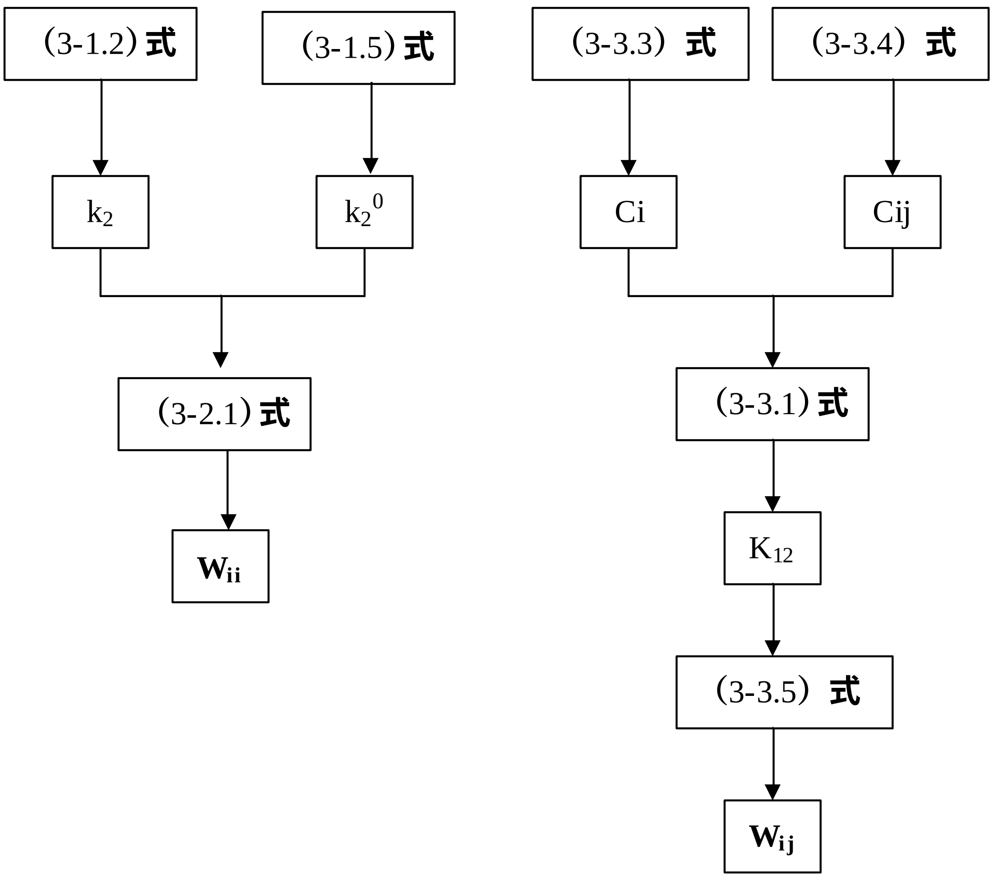

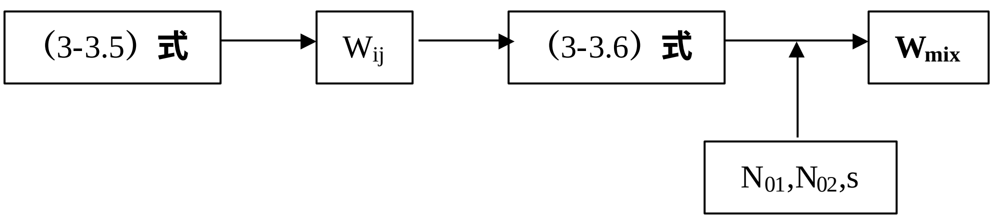

(三)不同重力不同粒徑膠體粒子混合的 N_G 值

表[G-1] 不同重力不同粒徑膠體粒子混合的 N_G 值

g-force / particle size	9.8 m/s^2	14.7 m/s^2	19.6 m/s^2
3.04 μm 6.2 μm	165.6	248.42	331.23
1.16 μm 6.2 μm	162.43	243.64	324.86
0.76 μm 6.2 μm	161.64	242.46	323.27
1.16 μm 3.04 μm	5.36	8.04	10.72
0.76 μm 3.04 μm	4.82	7.22	9.63
0.76 μm 1.16 μm	0.109	0.16	0.22

附錄 H

膠體溶液在顯微鏡 4000 倍下
膠體粒子膠凝之圖片

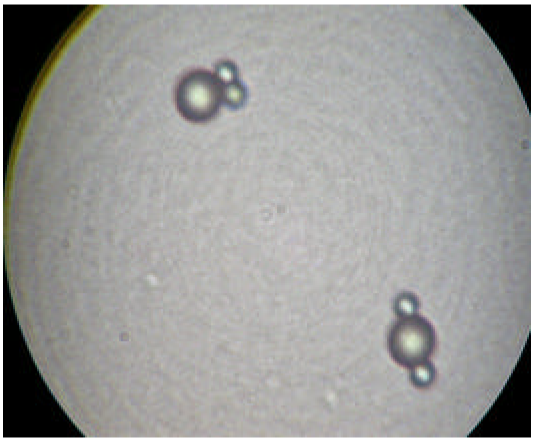

Fig[H-1] 10^{-4}M NaCl 6.2 μm+3.04 μm

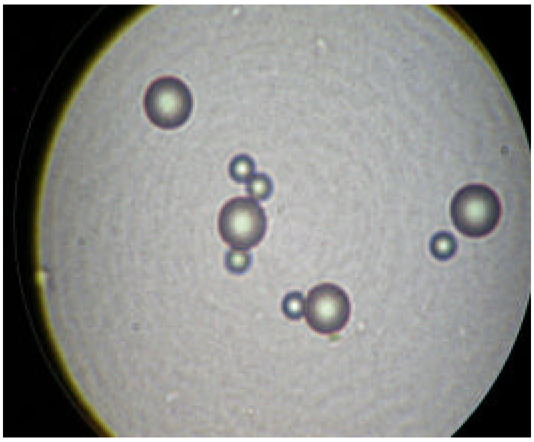

Fig[H-2] 10^{-3}M $MgCl_2$ 6.2 μm+1.1 μm

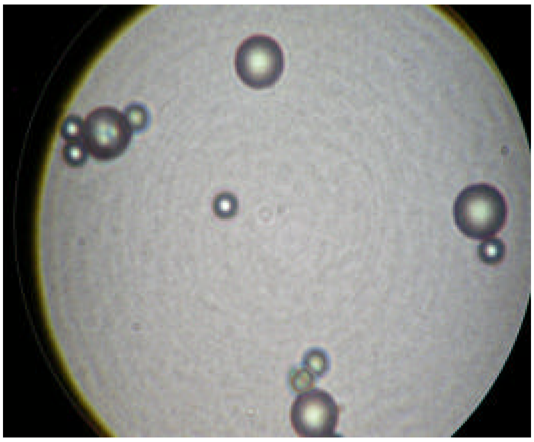

Fig[H-3] 10^{-4}M $AlCl_3$ 6.2 μm+3.04 μm

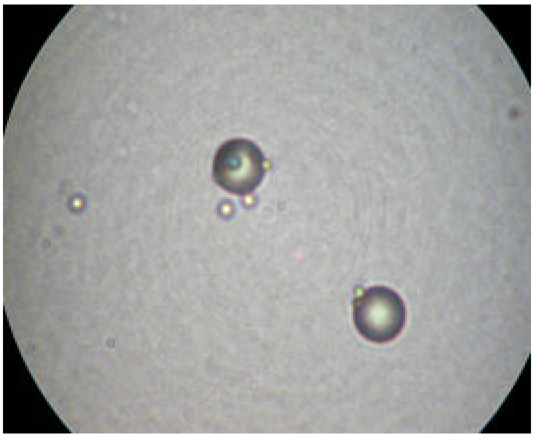

Fig[H-4] 10^{-3}M $AlCl_3$ 6.2 μm+1.1 μm

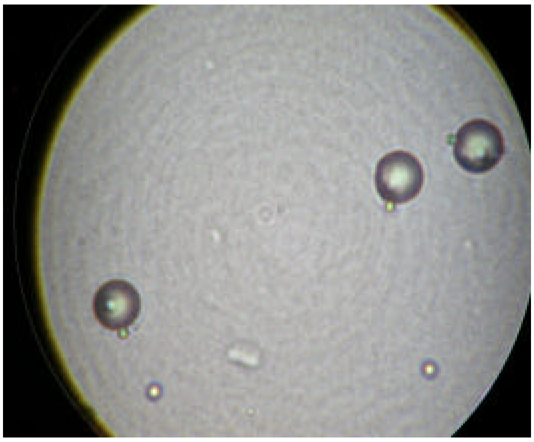

Fig[H-5] 10^{-4}M $MgCl_2$ 6.2 μm+0.807 μm

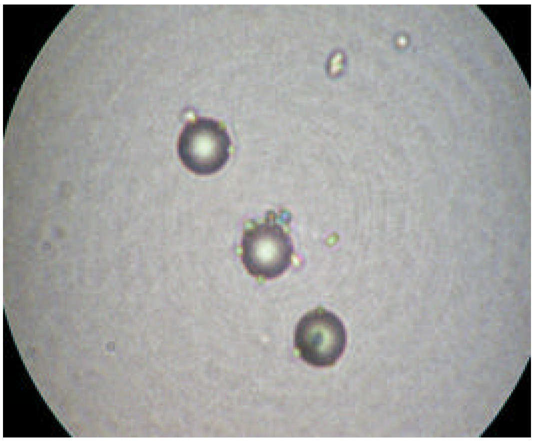

Fig[H-6] 10^{-4}M $AlCl_3$ 6.2 μm+0.807 μm